

國立交通大學

顯示科技所

碩士論文

交流電漿顯示器之氧化鎂層衰退與烙痕現象之
研究



Degradation of MgO thin films and Image Sticking

Phenomenon in AC-PDP

研究生：任珂銳

指導教授：金星吾 教授

中華民國九十五年七月

交流電漿顯示器之氧化鎂層衰退與烙痕現象之研究

Degradation of MgO thin films and Image Sticking
Phenomenon in AC-PDP

研究生：任珂銳

Student：Ko-Ruey Jen

指導教授：金星吾

Advisor：Sung-O Kim



碩士論文

A Thesis
Submitted to Display Institute
College of Electrical Engineering
National Chiao Tung University
in Partial Fulfillment of the Requirements
for the Degree of Master
In
Display Institute
June 2006
Hsinchu, Taiwan, Republic of China

中華民國九十五年七月

交流電漿顯示器之氧化鎂層衰退與烙痕現象之研究

學生：任珂銳

指導教授：金星吾 助理教授

國立交通大學顯示科技所研究所碩士班

摘 要

交流電漿顯示器中的氧化鎂保護層是用來保護介電層，延長電漿顯示器壽命的重要材料。氧化鎂保護層同時有很高的二次電子產生係數，因此可以降低驅動電壓，達到減少耗電量的效果。在這篇論文裡，我們利用一系列的壽命測試，來研究螢光體對氧化鎂保護層的影響。我們發現紅色螢光體比其他的螢光體更快速地使電漿顯示器的驅動電壓範圍縮小，因此推論紅色螢光體對氧化鎂層的壽命有較大的影響。在後續的表面材料分析中，在氧化鎂層中發現了紅色螢光體的組成元素鈮（Yttrium），與之前的推論相符。

電漿顯示器最為人詬病的烙痕問題，是由一靜止不動，連續長時間顯示的影像所造成。烙痕現象可分為永久性與暫時性的，我們改變電漿顯示器中填充的惰性氣體設定，來研究不同設定對暫時性烙痕現象的影響。結果顯示，雖然高氬氣和高氣體總壓的設定能提高面版的發光亮度，但是也會造成較為嚴重的烙痕現象。

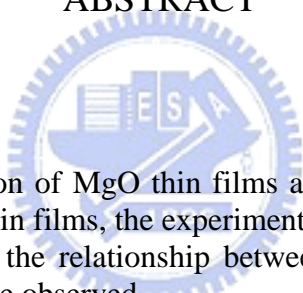
Degradation of MgO thin films and Image Sticking Phenomenon in AC-PDP

Student: Ko-Ruey Jen

Advisors : Prof. Sung-O Kim

Display Institute
National Chiao Tung University

ABSTRACT



In this study, the degradation of MgO thin films and image sticking phenomenon were investigated. For MgO thin films, the experiment focus on the contaminations by phosphor. For the other part, the relationship between image sticking phenomenon and inert gas mixture ratio were observed.

MgO thin film is one of the most important materials in an ac-PDP. It has high secondary electron emission coefficient and high sputter resistance, which decrease firing voltage and increase the life time of ac-PDP, respectively. The phosphors are related to luminance and color performance.

The lifetime tests for degradation of MgO thin films in ac-PDP were proposed. The driving margin is directly related to properties of MgO thin films. The variation of driving margin is observed as a function of time. After long time operation, the panels with red phosphor have an obvious degradation in driving margin area. An accelerated lifetime test was performed for a vertical discharge type one. The surface morphology and contaminations in the MgO thin films were investigated. By XPS, it is confirmed that the element Yttrium, which is one of the main elements in the red phosphor, is contaminated in the MgO thin films of the vertical discharge type panel. It revealed that the degradation of the MgO thin films in AC-PDP was partially caused by contaminations from phosphor.

Image sticking phenomenon is a critical issue in ac-PDP. An image sticking observation of 46 inch WVGA AC-PDP was performed. The luminance degradation related to white image sticking phenomenon was investigated. The white image sticking phenomenon become more serious as a function of Xe concentration (6%, 9%), and total pressure (475 torr, 550 torr).

誌 謝

首先，感謝指導教授金星吾教授兩年來的指導，提供良好的學習環境讓我能專心投入研究工作，此外，老師在語言能力上的要求，也讓我努力去加強，在做人處事上也都有明顯的進步，並且學到很多寶貴的技术和經驗。

兩年的碩士生活中，非常感謝實驗室同學李偉誠、周鴻杰、吳振宇和卓龍財的幫忙，除了在研究過程中提供許多參考，更訓練我獨立思考問題的能力，從分析問題中去尋找解決的方法，學習過程中的點點滴滴，對我都是很好的訓練。此外，非常感謝中華映管公司提供材料和設備，還有陳孝生處長、建邦學長、志明學長、建興學長提供的協助，對我而言，實在是難得的機會，這樣的合作，讓我看到業界和學界的差異，更加要求效率和實用性，在這過程中的訓練，對我而言，是非常可貴的。

再者，也要感謝工研院的周有偉先生，交大材料所的蔡志豪學長與王威超學長在材料分析上的協助與諮詢。實驗室的林義淵和楊子民學弟以及助理雅惠小姐，也使我的生活充滿了歡笑和回憶。最後，更要特別感謝父母親、家人對我的關懷，給我最大的支持和鼓勵，使我能夠專心的進行研究，在此敬上我最誠摯的敬意與感謝。

Table of Contents

Abstract (Chinese)	i
Abstract (English)	ii
Acknowledgements	iii
Table of Contents	iv
Table Caption	vi
Figure Caption	vii
<i>Chapter 1 Introduction to Plasma Display</i>	1
<i>Chapter 2 Principle of AC-PDP</i>	6
2.1 Introduction of Plasma	6
2.2 Cell Structure of the Plasma Display Panel	8
2.3 Driving Method	9
2.4 Gas discharge characteristics of Xe-Ne mixture	12
<i>Chapter 3 Recent Research for Plasma Display</i>	21
3.1 Image Sticking Phenomenon	21
3.1.1 White TIS Observation.....	23
3.1.2 Temperature dependence characteristic of the image sticking phenomenon.....	25
3.1.3 New Driving Method to Reduce Background TIS.....	30
3.1.4 Summary.....	31
3.2 Influence of Xe-Ne inert gas ratio	32
3.3 MgO and Phosphor Doping and Contamination	34

<i>Chapter 4 Investigation Method and Experimental Setup</i>	42
4.1 Motivation and Investigation Method	42
4.2 Measurement System	43
<i>Chapter 5 Results and Discussion</i>	46
5.1 Variation of Driving Margin	46
5.2 Contamination of MgO thin films by Phosphors in AC-PDP	51
5.2.1 Experiments.....	51
5.2.2 Results and Discussion.....	53
5.2.3 Summary.....	55
5.3 Observation of Image sticking with different Xe partial pressure and Total Inert Gas Pressure	55
5.3.1 Experiments.....	55
5.3.2 Result.....	56
5.3.3 Summary.....	64
<i>Chapter 6 Conclusion</i>	65

Reference

Table Caption

Tab. 3.1 The specific data of the phosphors.....	40
Tab. 5.1 Experimental PDP Setup.....	47
Tab. 5.2 Experimental PDP Setup.....	56



Figure Caption

Fig. 1.1 Features of Plasma Display.....	2
Fig. 1.2 The world's largest 103 inch Plasma Display made by Matsushita.....	3
Fig. 1.3 The application of Plasma Display.....	4
Fig. 2.1 Schematic Diagram of Gas Discharge Phenomenon.....	7
Fig. 2.2 Typical cell structure of the AC-PDP.....	9
Fig. 2.3 Typical cell structure of the AC-PDP.....	9
Fig. 2.4 Schematic diagram of sub-field.....	12
Fig. 2.5 Energy state of Xenon.....	16
Fig. 2.6 Stripe type barrier rib for AC-PDP.....	18
Fig. 2.7 The waffle structure of PDP cells.....	18
Fig. 2.8 Wavelength of UV, visible light and Infrared.....	19
Fig. 3.1 shows the image sticking phenomenon after 4 h pattern displayed.....	22
Fig. 3.2 shows the luminance difference between the image sticking cell and non image sticking cell after 5 min square-shaped pattern displayed.....	22
Fig. 3.3 Luminance difference for the unsealed test panel experiment.....	23
Fig. 3.4 Time-dependent Visible/IR emission intensity.....	24
Fig. 3.5 (a) Original square-shaped white image patterns displayed for 15 min and luminance degradation and rise in cell temperature with variations in gray levels during 30-min sustain discharge, (b) image sticking patterns on bright background, (c) image sticking patterns on dark background, and (d) image sticking patterns at low-sustain voltage.....	26
Fig. 3.6 (a) IR waveforms emitted from discharge cells including cell temperature rise as function of display time and (b) IR recovery characteristics.....	27
Fig. 3.7 (a) Changes in IR waveforms emitted from cells adjacent discharge cells	

including cell temperature under white image pattern during ramp reset-period as function of display time, and (b) IR recovery characteristics.....	28
Fig. 3.8 Changes in IR waveforms emitted from cells during ramp reset-period when the front panel is heated by heater at various temperatures.....	29
Fig. 3.9 New driving method for reducing background ITS.....	30
Fig. 3.10 Background luminance of OFF cells for proposed and conventional driving method.....	31
Fig. 3.11 Dependence of luminous efficiency for several Xe partial pressures (Total pressure: 667hPa).....	33
Fig. 3.12 Dependence of firing voltage (Vf) and minimum sustaining voltage (Vsm) for several Xe partial pressures (Total pressure: 667hPa).....	33
Fig. 3.13 SEM images of the AC-PDP micro cell structure.....	35
Fig. 3.14 Spatial variation of the MgO surface in the a.c.-PDP.....	36
Fig. 3.15 SEM images of a virgin a.c.-PDP and two other ones operated for 9 and 1000 h, respectively.....	37
Fig. 3.16 3-Dimensional surface profiles of the MgO-layer in a PDP-cell.....	38
Fig. 3.17 The normalized-thickness curves vs. lateral position.....	38
Fig 3.18 Secondary electron emission coefficient (γ) of MgO thin films with different degraded condition.....	39
Fig. 3.19 Change of MgO protective layer before and after discharge.....	39
Fig. 4.1 Electrical and optical measurement system.....	44
Fig. 4.2 X-ray Photoelectron Spectroscopy (XPS), VG Scientific, Microlab 350.....	45
Fig. 5.1 The driving margin of the panel with red phosphor KX504A after (a) 18 hour and (b) 1000 hour accelerated test time (aging).....	49
Fig. 5.2 The driving margin of the panel with red phosphor NP360-53 after (a) 18	

hour and (b) 1000 hour accelerated test time (aging).....	49
Fig. 5.3 The driving margin of the panel with green phosphor P1G1S after (a) 18 hour and (b) 1000 hour accelerated test time (aging).....	49
Fig. 5.4 The driving margin of the panel with green phosphor NP200-205 after (a) 18 hour and (b) 1000 hour accelerated test time (aging).....	49
Fig. 5.5 The driving margin of the panel with blue phosphor NP107-343 after (a) 18 hour and (b) 1000 hour accelerated test time (aging).....	50
Fig. 5.6 The driving margin of the panel with blue phosphor LG Chem after (a) 18 hour and (b) 1000 hour accelerated test time (aging).....	50
Fig. 5.7 The driving margin of the panel with RGB phosphor after (a) 18 hour and (b) 1000 hour accelerated test time (aging).....	50
Fig. 5.8 The driving margin of the panel with RGB phosphor after (a) 18 hour and (b) 1000 hour accelerated test time (aging).....	50
Fig. 5.9 Schematic diagram of the surface sustain discharge and vertical sustain discharge.....	51
Fig. 5.10 (a) AFM images of MgO thin films vertical discharge type panel after 700-hour accelerated test time. (b) AFM images of surface discharge type panel after 16000-hour accelerated test time.....	53
Fig. 5.11 (a) XPS surface analysis of the vertical discharge type panel after 700-hour accelerated test time. (b) XPS surface analysis of the surface discharge type panel after 16000-hour accelerated test time.....	54
Fig. 5.12 (a) Photo diagram of the applied pattern (b) Photo diagram of the White Image sticking Phenomenon (c) Photo diagram of the Dark Image sticking Phenomenon.....	56
Fig. 5.13 Luminance degradation as a function of sustain time.....	57
Fig. 5.14 Luminance degradation of the (a) red cells (b) green cells (c) blue cells as a	

function of sustain time. Color temperature variation as a function of full white display time.....58

Fig. 5.15 Luminance degradation of the PDP after different pattern sustain time.....61

Fig. 5.16 Recovery ability of the panels with (a) 30 sec pattern sustain time. (b) 1 min pattern sustain time. (c) 2 min pattern sustain time. (d) 5 min pattern sustain time. (e)10 min pattern sustain time.....62



Chapter 1 Introduction to Plasma Display

Cathode Ray Tube is the most common display in the world. It has been developed for 80 years and its technology is well developed. However, due to the display theory of CRT, it is heavy and large when the display size increases. Thus the conventional size of CRT in the market is limited to about 30 inch, and the largest one is about 50 inch, which is extremely heavy and large. The flickering effect and radiation issue also are taken notice by consumers. Due to the disadvantages listed above, further development of CRT display is limited. Thus in recent years, people pay attention on the Flat Panel Display (FPD).

Plasma display panels are one of the leading candidates in the competition for large-size, high-brightness, high contrast ratio flat panel displays, suitable for high definition television (HDTV) wall-mounted monitors. Their advantages include large screen size, wide viewing angle, low weight, small thickness and simple manufacturing process for fabrication, as shown in Fig 1.1. The plasma display panel was invented at the University of Illinois at Urbana-Champaign by Donald L. Bitzer and H. Gene Slottow in 1964 for the PLATO Computer System. In 1983, IBM developed a 19" orange on black monochrome display. In 1992, Fujitsu introduced the world's first 21-inch full color display. In early years, PDP application was limited to industry due to its high price. Plasma's relatively large screen size and thin profile made the displays attractive for lobbies and stock exchanges. In 1997 Pioneer started selling the first plasma television to the public. With the development and manufacture of many companies, the size of PDP grows bigger and bigger. In recent years, the improvement of technology makes PDP great image quality, which approaches the traditional CRT.

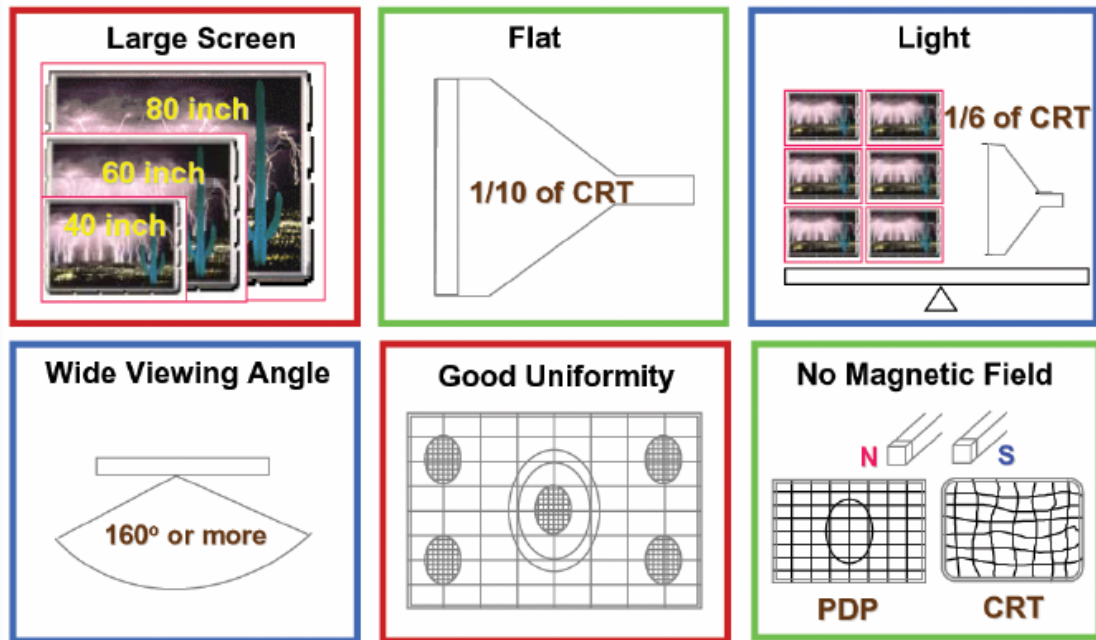


Fig. 1.1 Advantages of Plasma Display

Due to the theory and manufacturing process of AC-PDP, it is suitable to make large size flat panel display. Screen sizes have increased since the Fujitsu's 21 inch display in 1992. Right now the conventional size is between 42 inch to 55 inch, and 71 inch size is already in production. The largest plasma display in the world was shown at the CES (Consumer Electronics Show) in Las Vegas in 2006. It is 103 inch and was made by Matsushita Electrical Industries (Panasonic), as shown in Fig. 1.2.



Fig 1.2 The world's largest 103 inch Plasma Display made by Matsushita

Plasma displays have high contrast ratio, wide viewing angle, fast response time, good color performance and can be produced in very large sizes up to 103 inches. High dark-room contrast makes the PDP suitable for watching movies. Since each pixel is lighted individually, the image is very bright and looks good from almost every angle. The power consumption per square meter of plasma displays is as much as a CRT TV. Real life measurements indicate 150 Watts for a 50 inch PDP. The lifetime of the new generation plasma displays is about 60,000 hours. Precisely, it is the estimated half life of the PDP. Half life is the point where the brightness has degraded to half of its original value, which is considered the end of the life of the display. So a plasma display will last approximately 20 years if it is viewed 8 hours a day.



Fig 1.3 The application of Plasma Display

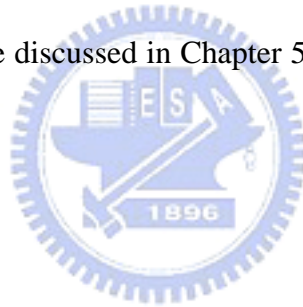
The superior brightness and wider viewing angle of color plasma displays, when compared to LCD televisions, made them one of the most popular forms of display for HDTV. Right now the TFT-LCD dominates the market below 40 inch while PDP dominates that above 40 inch. With the competition of the large size TFT-LCD, it is very important for PDP manufacturers to improve luminous efficiency, solve image quality issue and lower the price to occupy the market of large size flat panel display.

In 2005 the cost has come down to NT\$50000 or less for the popular 42 inch diagonal size, making it very attractive for home-theatre use. In US, many of the retailers reported that plasma TVs were among the hottest selling items for Christmas season in 2005. As of early 2006, sales of plasma TVs and LCD TVs combined exceeded sales of CRT TVs for the first time.

Recent progress for PDP technology development and manufacturing has been remarkably improved. However, there are many problems that need to be resolved. One of the most critical issues in PDP research is the improvement of the luminance and luminous efficiency of the display, which are low compared to conventional

cathode ray tube displays (CRTs). Another important problem is the relatively high operating voltages which increase the cost of the electronics and consequently the overall cost of the display. Finally there are some image quality issue like dynamic false contour[1] and image sticking phenomenon[2].

This research will focus on two major aspects. One is the degradation and contaminations of the MgO thin films caused by phosphors. The other is the influence of the noble gas mixture on the image sticking phenomenon. In Chapter 2, the principles of PDP will be introduced. Recent research about image sticking phenomenon, MgO thin film, Phosphor and gas mixture of PDP will be reviewed in Chapter 3. Chapter 4 will introduce the experiment setup and investigation method. The result in this study will be discussed in Chapter 5. Finally, the conclusion will be given in Chapter 6.



Chapter 2 Principle of AC-PDP

2.1 Introduction of Plasma

Plasma is one of the greatest discoveries in the Modern Physics. The gas molecule is converted to the partial ionized gas resulted from the collision or excitation by the particles with high energy, such as light, radioactive rays and electrons. This partial ionized gas consists of charged particles like electrons, ions, excited molecules, and neutral molecules and atomic group. This is what we call “plasma.” It is different from the solid state, liquid state and gas state and is called the fourth state of substance. The act of individual electron in plasma looks like disorderly but the whole electrons act as a group. It is the characteristic of plasma. It appears to be neutral charged inside plasma, which means that the density of negative charged particles is the same as that of positive charged particles.

To generate plasma, apply an electric field first. Electric field can provide energy and high velocity for electrons in gas. When the non-charged particle is collided with accelerated electrons, one ion and another accelerated electron are generated. These electrons are also accelerated by electric field then collide with other neutral particles. The plasma state is formed by repeating this process continuously and generate large amount of electrons and ions in a short time. This phenomenon is called Gas Breakdown effect, as Fig. 2.1 shows.

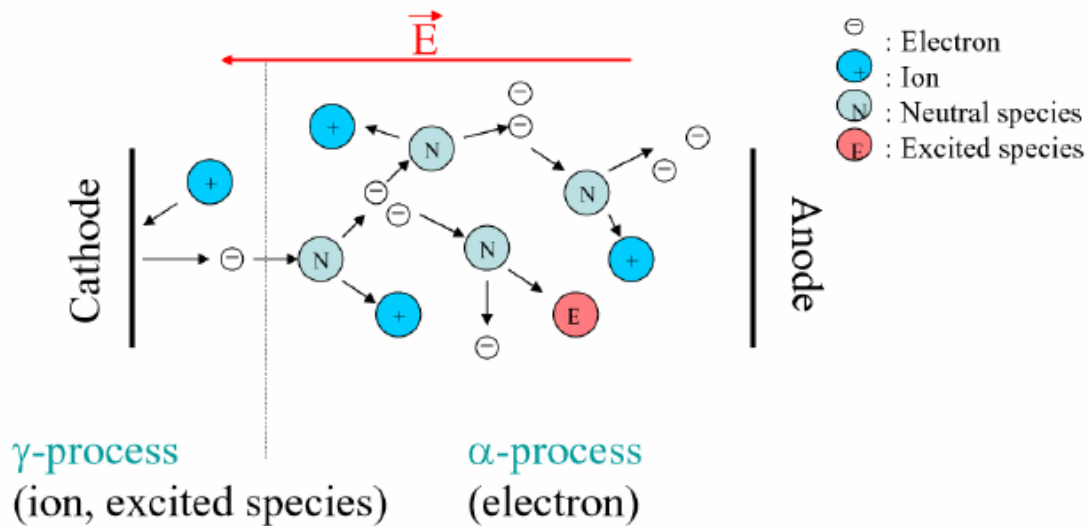


Fig. 2.1 Schematic Diagram of Gas Discharge Phenomenon

The particles in this section carry electric charge and result in static electric force between each other. Thus the case is different from the model described by the classical physics. That is to say, the energy transfer between the particles is not necessarily done by “touch.” As the distance between the particles approaches the specific range of collision cross section, the path and energy are influenced with each other just like the real collision.

Scientists use the plasma technology to improve the daily life of people. The most successful and common product is the fluorescent lamp and the neon lamp. When we push the button, the igniter generates extremely high voltage and produce plasma. The particles in plasma will bombard the mercury vapor and phosphorous layer, thus the lamp is light up. By efforts of scientists, more and more products using plasma technology are successfully developed. However, this doesn't represent the technique and theory involved is fully understood. Plasma display is one of the examples. Therefore, to continue research on the emissive characteristic and theory of plasma display is one way could not be ignored.

2.2 Cell Structure of the Plasma Display Panel

Typical color plasma display consists of two glass plates, each with parallel electrodes deposited on their surfaces, as shown in Fig. 2.2. The most common type of color plasma display is the coplanar-electrode PDP. In this PDP type, each cell is formed by the intersection of a pair of transparent sustain electrodes X and Y (usually made of transparent conductive material, ITO) on the front plate, and an address electrode A (usually made of metal) on the back plate. A bus electrode made of metal is attached to each ITO electrode. Since the resistivity of ITO is not zero and the length of the electrodes can be very large, the metal bus electrode can maintain constant potential along the ITO electrodes. The electrodes are covered with dielectric films typically made of enamel or aluminum. A protective MgO layer is deposited above the dielectric film on the front plate. The role of this layer is to protect the dielectric film from ion bombardment and decrease the breakdown voltage due to the relatively high secondary electron emission coefficient of MgO. On the back plate barrier ribs are formed, which separate both electrically and optically adjacent cells with different colors. In each cell phosphors are deposited that emit one primary color, red, green, or blue. Each PDP pixel consists of three adjacent cells. The two plates are sealed together with their electrodes at right angle, and the gap between the plates is first evacuated and then filled with an inert gas mixture. When sufficiently high voltages are applied to the electrodes of the PDP cell, breakdown occurs which results in ionization and UV emission. Some of the UV photons emitted by the discharge hit and excite the phosphors deposited on the walls of the PDP cell. The phosphors emit visible photons, some of which come out of the front plate and reach the observer.

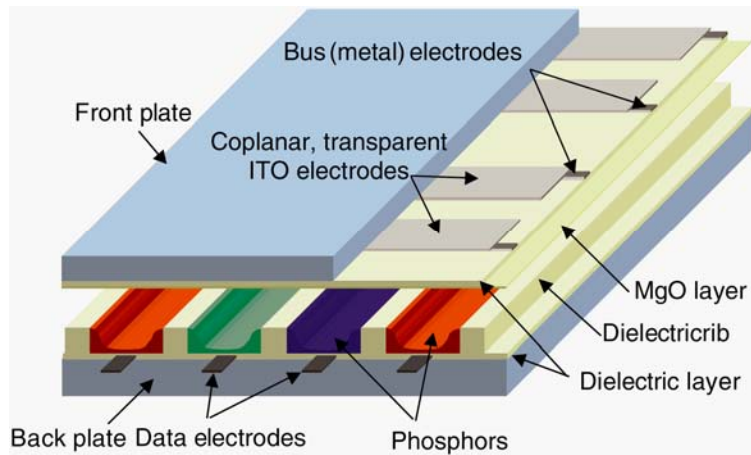


Fig. 2.2 Typical cell structure of the AC-PDP

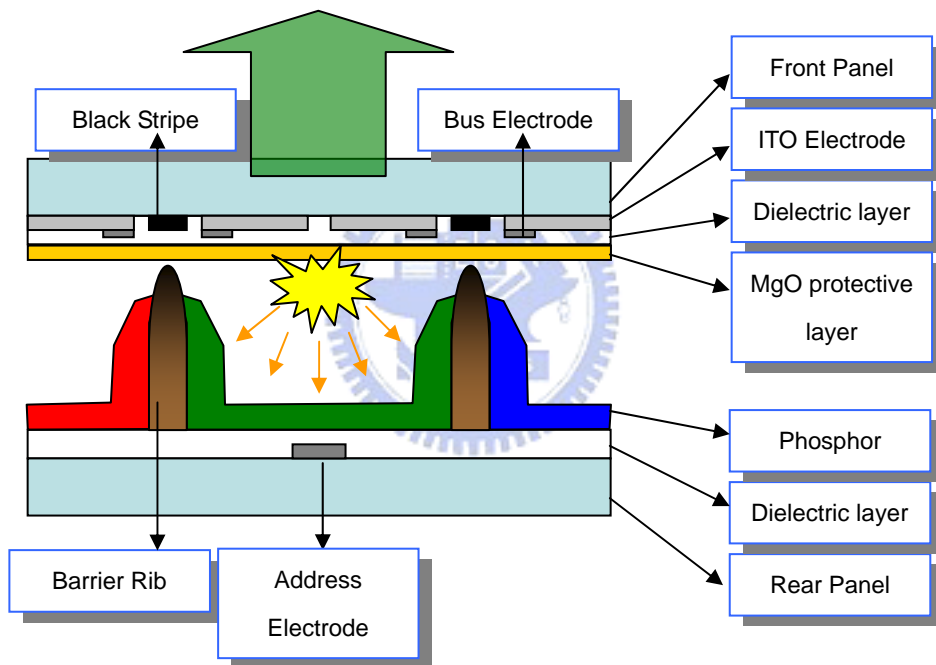


Fig. 2.3 Typical cell structure of the AC-PDP

2.3 Driving Method

As we mentioned above, the two plates are sealed with their electrodes at right angles, so that one of the two plates shown in Fig. 2.3 has to be rotated by 90 degree. PDP cells are formed at intersection of electrodes on the front and back plates. The conventional driving method of the plasma display is the address display separated

(ADS) method, which consists of three phases: the reset phase, the addressing phase, and the sustaining phase. First the cells are reset at reset phase. During the addressing phase, scan pulses are applied successively to each one of the parallel Y sustain electrodes, also known as scan electrodes. During the application of the scan pulse at a specific line of the display, data pulses are applied only to those address electrodes which correspond to cells in that specific line which have to be turned on. The application of the scan voltage pulse and of the data pulse on the scan and address electrodes respectively results in an electrical field E in the gap between the two dielectrics sufficient to cause breakdown. The discharge results in ionization and consequently production of positively and negatively charged particles, ions and electrons. Positive and negative charges move under the influence of the applied electric field in opposite directions and accumulate on the walls of the dielectric layers. The electric field of the accumulated surface charge opposes the electric field of the applied voltage and the discharge is eventually quenched.

During the sustaining phase, sustain voltage are applied to the sustain electrodes in all cells. The electric field produced by the applied voltage is not enough to cause breakdown. However, in those cells that have been previously addressed, the electric field due to the applied voltage adds to the electric field induced by the accumulated surface charge, so that the total field is sufficient for breakdown. Positive and negative charges are again produced through ionization and move in opposite direction, until the electric field of the newly accumulated surface charge opposes the electric field of the applied voltage and the discharge is eventually quenched. However, on the next sustain cycle the sustain pulse is applied to the other sustain electrode so that the induced electric field of the surface charge accumulated on previous cycle adds onto the field. The discharge is again eventually quenched, and

the same process is repeated during the sustaining phase.

PDP cells can operate when the applied sustaining voltage V_s is held within certain limits known as the minimum sustaining voltage V_{smin} and the firing voltage V_f . The initial address pulses trigger a discharge between the address and scan electrode. The discharge is quenched by surface discharges accumulated on the dielectric layers. Subsequent sustain discharges occur only in the address cells, since the sustain voltage V_s is lower than the breakdown voltage as previously mentioned. The minimum sustaining voltage V_{smin} is defined as the minimum value of V_s which leads to a steady sequence of sustaining discharges in an addressed cell. The firing voltage V_f is defined as the breakdown voltage in an unaddressed cell. The sustaining voltage V_s must at all times be less than V_f in order to avoid discharges in cells which are not addressed. The voltage margin of the cell is thus defined as range between V_f and V_{smin} . In real PDPs V_f and V_{smin} exhibit some variation, since cells have slightly different dimensions. The voltage margin of the cell should therefore be as large as possible to ensure reliable operation of the display.

In order to achieve color resolution, each TV field (with typical duration of 16.7 ms) is divided into eight subfields. Each subfield consists of an addressing and a sustaining phase. The duration of the sustaining phases in the different subfields are proportional to powers of 2 so that each one of them corresponds to one bit of resolution. That means, each subfield can be sustained for 1, 2, 4, 8, 16, 32, 64, 128 times a given number of discharge pulses. By combining any of eight subfields, 256 grey levels can be achieved, as Fig 2.4 shows. Sustain frequencies are typically 50~350 KHz, so that a very large number of sustain pulses occur during each TV field.

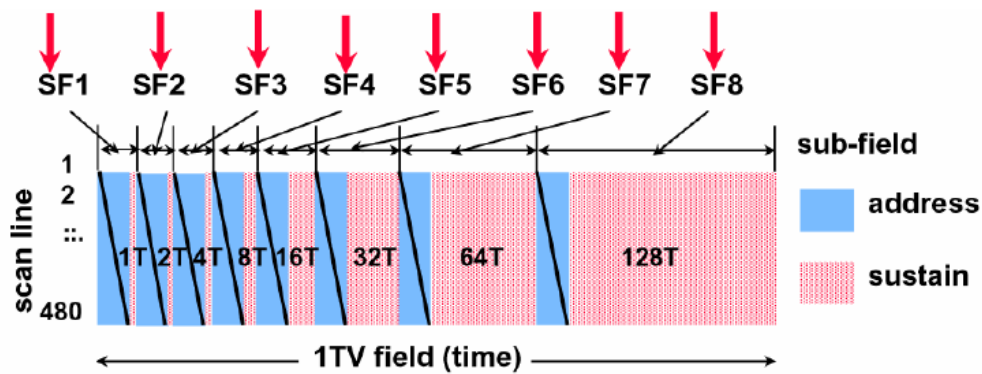


Fig 2.4 Schematic diagram of sub-field

2.4 Gas discharge characteristics of Xe-Ne mixture

In this section, the working mechanism of the plasma display, from plasma discharge to visible light emission, will be introduced. The working mechanism of the surface discharge plasma display can be divided into two parts.

(1) VUV production and propagation

Apply strong electric field to give rise to plasma discharge for generating Vacuum Ultra Violet (VUV). Then VUV propagates to phosphorus layer.

(2) Phosphor conversion and visible light emission

The phosphorous layer absorbs the energy and emits the visible light.

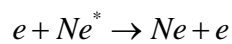
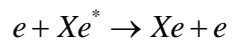
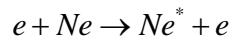
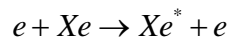
The total process includes VUV production and propagation, phosphor conversion, visible light emission and loss. From this procedure, we know that the plasma display uses the input power to generate VUV by gas discharge, and the VUV can excite the three different phosphor materials to emit the red, green and blue light. The luminous efficiency of the PDP depends on the efficiency of these four processes.

2.4.1 VUV Production and Propagation

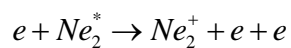
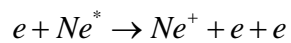
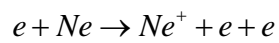
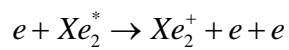
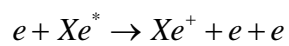
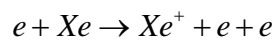
Because of the exceedingly small cells, the characteristic of gas discharge can not be observed directly. Also, the voltage and UV light in the discharge cells can not be measured directly. However, in order to improve the luminous efficiency of the plasma display, it is essential for us to understand the complex process of UV generation in the discharge cells. This, by models and theories from many researches, the principles of VUV generation can be understood.

For the conventional three electrode surface discharge AC-PDP, the gas mixture of Neon and Xenon inert gas are used as discharge gas in the cells. The concentration of Xenon gas is normally between 4%~10%. In some case, in order to improve the luminous efficiency, other inert gas is added to this mixture, such as Helium and Argon, etc. For this kind of setup, the dominate particles for the VUV emission in PDP application are from Xenon gas. When the high voltage difference is applied between the scan and sustain address electrode on the PDP front panel, the breakdown occurs. The main reactions in the cell are listed in the next page.

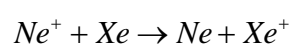
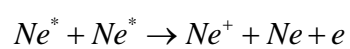
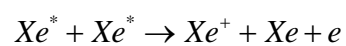
Electron Impact Excitation and De-excitation

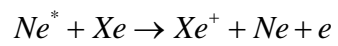


Electron Impact Ionization and Recombination

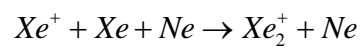
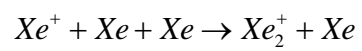
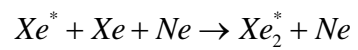
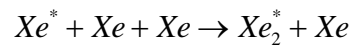


Two-Body Heavy Particle Collisions

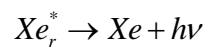
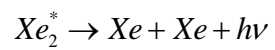




Three Body Heavy Particle Collisions



VUV Radiation



Base on the reactions listed above, the VUV emission can be acquired by the gas discharge. The light with 147 nm and 173 nm is the most important for the application on the plasma display. Figure 2.5 shows the energy levels of the main reactions.

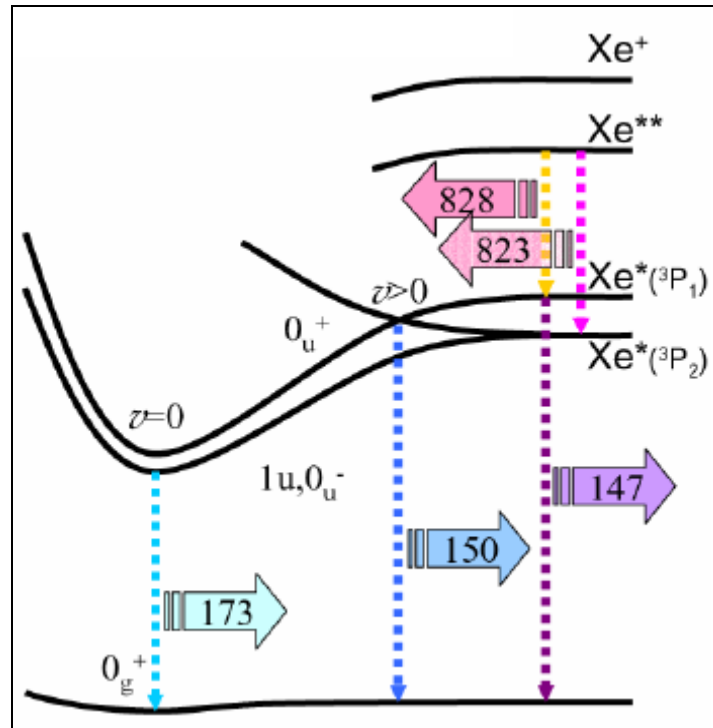


Fig 2.5 Energy state of Xenon

During the process of the VUV emission, roughly 30% of the input power is converted into heating of electrons, and 70% into heating of positive ions. Positive ion gets only several eV by the electric field, resulted from its heavier body. Because of the low energy, positive ion doesn't contribute much in the generation of VUV. Most of them collide with the surface structure and generate heat, which is the main source of waste energy. The kinetic energy of the electron can be transferred to generate VUV. The efficiency of this part is about 20%. As one can see, only a little part of input power is used as the energy to generate VUV, which means it is an important section needed to be improved.

In this step, about only 40% VUV emitted from the surface discharge can reach the phosphorous layer on the back panel for conventional structure of the surface discharge type AC-PDP. The VUV generated from the surface discharge center on the surface area of the dielectric layer on the front panel. There is a distance between the plasma near the front panel and phosphorous layer on the back panel. This design prevents from the directly ion bombardment from the plasma to phosphorous layer and increase the life time of AC-PDP. Thus the efficiency of VUV transport is necessary to improve.

The other factor involved in this issue is the position and area of printed phosphorous layer. It is very important to optimize the design of the cell structure to improve the luminous efficiency of the AC-PDP. When the surface area of the printed phosphorous layer increases, the rate of VUV absorbed increases. When the UV light increases, the emission of phosphor doesn't increase linearly because of long decay time of the phosphor materials. It is what we called phosphor saturation. Larger phosphorous area also prevents from phosphor saturation by decrease the load of unit phosphorous area and increase luminance and luminous efficiency.

The conventional discharge cell of AC-PDP is the stripe type, as shown in Fig. 2.6. For this type, phosphor is printed on the surface of dielectric layer and barrier rib. In order to increase area of printed phosphorous layer, it is essential to change the cell structure. Basically, the shape of discharge cell depends on the shape of barrier rib. Therefore, the design of the shape of barrier rib is very important because phosphor is printed on the vertical surface on the rib.

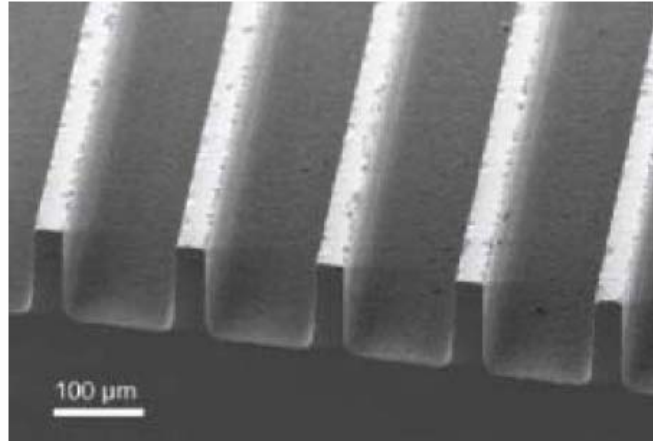
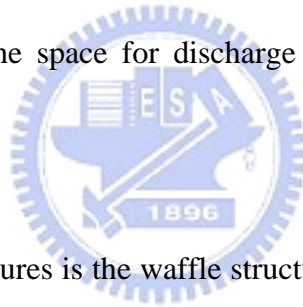


Fig. 2.6 Stripe type barrier rib for AC-PDP

Furthermore, the gas discharge must be restricted within the center area of the discharge cell in order to prevent from the cross talk phenomenon between the adjacent cells. Thus every two vertically adjacent cells have a dark area not allowed for gas discharge. It limits the space for discharge and visible light emission and should be improved.



One of the newer cell structures is the waffle structure as Fig 2.7 shows. Compared with the traditional stripe rib structure, waffle structure has the additional horizontal wall which can prevent cross talk between the vertically adjacent cells, and also has extra surface area for printed phosphorous layer, which improves luminous efficiency[3].

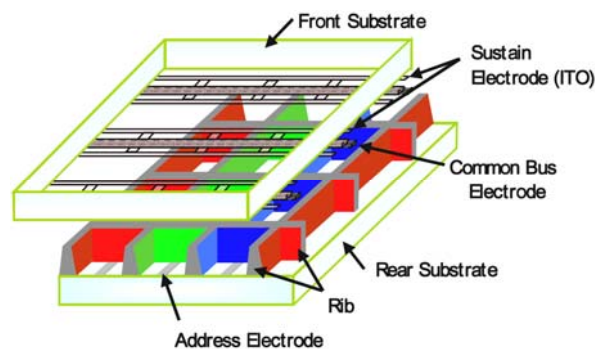


Fig. 2.7 The waffle structure of PDP cells [3]

2.4.2 Phosphor Conversion, Visible light emission and loss

The UV light and IR emission from the gas discharge in the PDP cells are not visible by human eyes. The UV light must be converted to visible light by special phosphor materials. The wavelength of visible light is between 380nm to 780nm. It includes red, orange, yellow, green, blue, indigo and purple. The light exceeded this range is not visible for normal human eyes. What we call infrared is the light with 780nm~1500nm wavelength, while the wavelength of UV light is shorter than 380nm. Fig. 2.8 shows the relationship between UV, visible light and infrared.

UV	Visible Light	Infrared
<300nm	400 nm~700nm	>800 nm

Fig. 2.8 Wavelength of UV, visible light and Infrared

The phosphorous layers are printed on the rear glass substrate of PDP. With three different kinds of phosphor materials, the UV light can be converted into red, green and blue light. By several kinds of address methods, the three colors can form all kinds of images with full color and different grey levels.

The efficiency of phosphor conversion deeply influences the luminous efficiency of the PDPs. Right now the quantum efficiency of the phosphor in used is almost over 0.8. One of the issues of the phosphor is the phosphor saturation. When the UV light increases, the emission of phosphor doesn't increase linearly because of long decay time of the phosphor materials. It is what we called phosphor saturation. To avoid this kind of phenomenon, it is necessary to choose phosphor materials with shorter decay time. Furthermore, the wavelength of the visible light is longer than that of UV light.

The visible/UV photon energy ratio is less than 1.

The UV light is converted to visible light by phosphorous layer on the PDP back panel. In order to be observed by human eyes, the visible light has to pass through many layers, such as MgO protective layer, Dielectric layer, ITO transparent electrode, glass substrate on the front panel, and anti-reflection layer, IR filter, anti electromagnetic interference layer, color compensation layer, etc. Because of these layers, the loss of visible light is serious. Even though each layer has 90% transparency, the efficiency of visible light output is only 40%.

As one can see, the efficiency in these processes is not good enough, especially the efficiency of the VUV light production. Thus the improvement of efficiency at these parts is essential for PDP to make lower power consumption.



Chapter 3 Recent Research for Plasma Display

In this chapter, the researches related to this study will be reviewed. This chapter is classified into three parts: In section 3.1, recent research on image sticking phenomenon. Influence of noble gas mixture will be discussed in section 3.2. In section 3.3, doping and contamination of MgO and phosphor will be introduced. Finally, a conclusion is given.

3.1 Image Sticking Phenomenon

There are many technical problems to overcome for plasma display, such as luminance efficiency, power consumption, lifetime and dynamic false contours, etc[1]. Among them, the most critical issue is the image sticking phenomenon, which is the ghost image that remains in a subsequent image when the previous image was continuously displayed over a few minutes. When the patterned static image is displayed for several minutes, recognizable ghost image of previous pattern is often observed in both background and full white display.

For instance, Fig. 3.1 (a) shows that the characters “PDP” continuously displayed for 4 hour on a 42-inch PDP-TV. When the “PDP” image was abruptly changed to a completely dark background or white background, the “PDP” image still remains on the dark (b) and bright (c) images, respectively. In Fig. 3.2, a similar result is obtained after a square-shaped white image was displayed for 5 min with 255 gray levels on a dark background. In the Fig. 3.1(b) and Fig. 3.2 (b), the luminance of the adjacent cells is observed to be higher than the luminance of both the cells with an image sticking and no image sticking. It is so called background image sticking. In the Fig.

3.1(c) and Fig. 3.2 (c), the luminance of the image sticking cells is lower than the no image sticking cells and is called white image sticking phenomenon. The image sticking phenomenon can recover with time (temporal image sticking, TIS) or last forever. If image sticking results from the MgO surface, this is related to the discharge current and IR emission. Conversely, if the problem results from the phosphorous layer, it is related to the luminance, cell temperature, and color coordinates of the red, green, and blue phosphor. In this section, recent research of image sticking will be arranged and discussed.

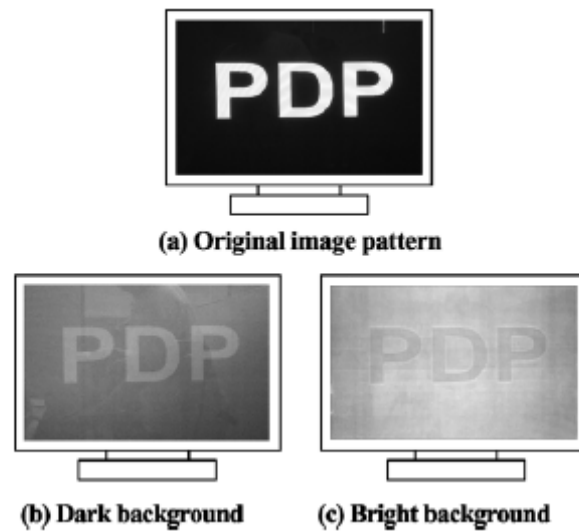


Fig. 3.1 shows the image sticking phenomenon after 4 h pattern displayed

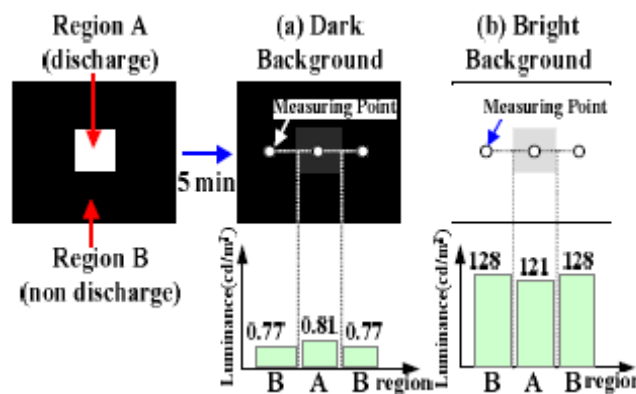


Fig. 3.2 shows the luminance difference between the image sticking cell and non image sticking cell after 5 min square-shaped pattern displayed. [14,4]

3.1.1 White TIS Observation

As describe in previous section, the region where peak white (from a small area static image) has been displayed become darker compared with the other cells experienced reset discharge only.

To find out the origin of white TIS, Ho-Jun Lee performed an unsealed test panel experiment in the UHV chamber. Upper plate of the panel was shifted after performing sustaining discharge in selected area as shown in the Fig. 3.3. This made three different regions. Region A corresponds to previously discharged phosphor with non-discharged MgO, B to previously discharged phosphor and MgO, C to non-discharged phosphor with discharged MgO. The results are shown in Fig. 3.3 Region A shows lowest luminance while region C shows highest luminance. This result implies that phosphor degradation is mainly responsible for decrement of luminance in white TIS.

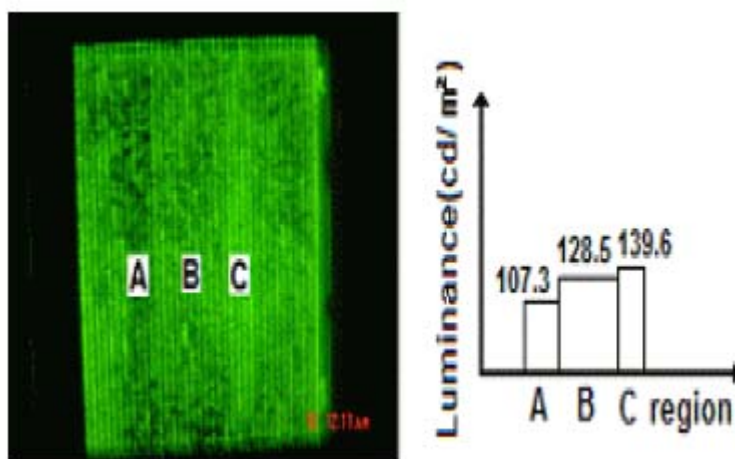


Fig 3.3 Luminance difference for the unsealed test panel experiment [5]

Fig. 3.4 shows intensity variation of visible and IR emissions during sustaining discharge. Visible emissions decreased rapidly up to 15 minutes and saturate. Intensity reduction of R, G and B cell was found to be 9.7, 11.1 and 11.8% respectively. On the other hand IR emission (823, 828nm) decreased only 2-3%. The 823, 828nm lines are emitted from the transition of $Xe^*(2p5)$ to $Xe^*(3P1)$ and $Xe^*(2p6)$ to $Xe^*(3P2)$. Since $Xe^*(3P1)$ and $Xe^*(3P2)$ are source and precursor of UV lights, IR emission is good indications of UV emission. This result also supports that white TIS is mainly related to phosphor degradation rather than the alteration of plasma characteristics. Another important point is that the reduction rate of emission intensity of each R, G, B is not identical. This produces shift of color temperature, which is very well recognizable in human eyes.

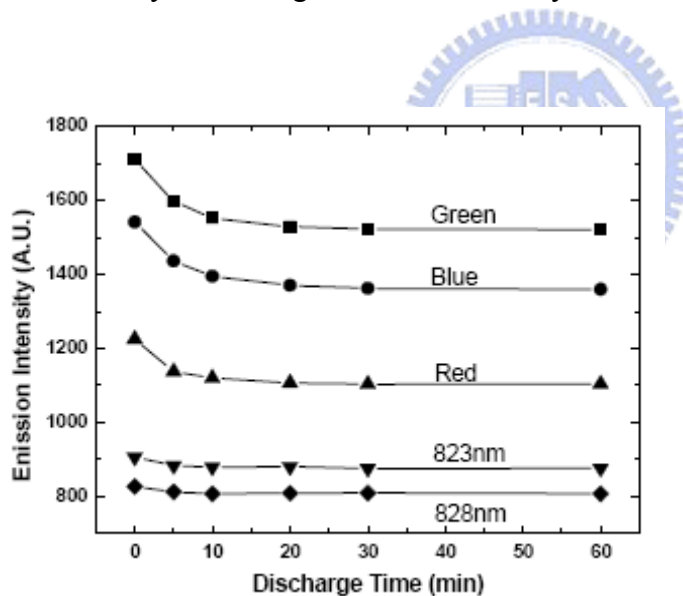


Fig. 3.4 Time-dependent Visible/IR emission intensity [5]

3.1.2 Temperature dependence characteristic of the image sticking phenomenon

Heung-Sik Tae performed a series of experiment to characterize the temperature dependency of temporal image sticking phenomenon. Fig. 3.5 (a) shows five white square images with different gray levels from 50 to 255, where the images were maintained for 15 min at a sustain voltage of 176 V. As seen on the right side of Fig. 3.5 (a), since the duration of the discharge increased with the gray level, the rise in the cell temperature was more serious in proportion to the gray level, making the decrease in the luminance more serious in proportion to the gray level. When the previous square image patterns in Fig. 3.5 (a) were abruptly changed to a completely bright subsequent image, five ghost images appeared, as shown in Fig. 3.5 (b), with the ghost image of the brightest previous square image appearing as the darkest ghost image. Similarly, when the previous square image patterns in Fig. 3.5 (a) were abruptly changed to a completely dark subsequent image, five ghost images also appeared, as shown in Fig. 3.5 (c), yet in this case, the ghost image of the brightest previous square image appeared as the brightest ghost image. As such, the results in Fig. 3.5 (b) and (c) indicate that the image sticking problem was more serious when the previous image was brighter. Meanwhile, Fig. 3.5 (d) shows the image pattern that appeared when the sustain voltage was abruptly reduced below the minimum sustain voltage on bright background after the previous image in Fig. 3.5 (a) was displayed for 15 min. In the regions with no image sticking, the discharge was completely turned off, as the low voltage, below the minimum sustain voltage, did not produce any discharge. However, the pattern of the previous image, i.e. the ghost image, still remained even at a reduced sustain voltage of 157 V, indicating a brighter luminance in proportion to the gray level. The discharge in just the image-sticking cells under a low-sustain voltage was presumably due to a change in the MgO surface that was more activated in proportion to the gray level.

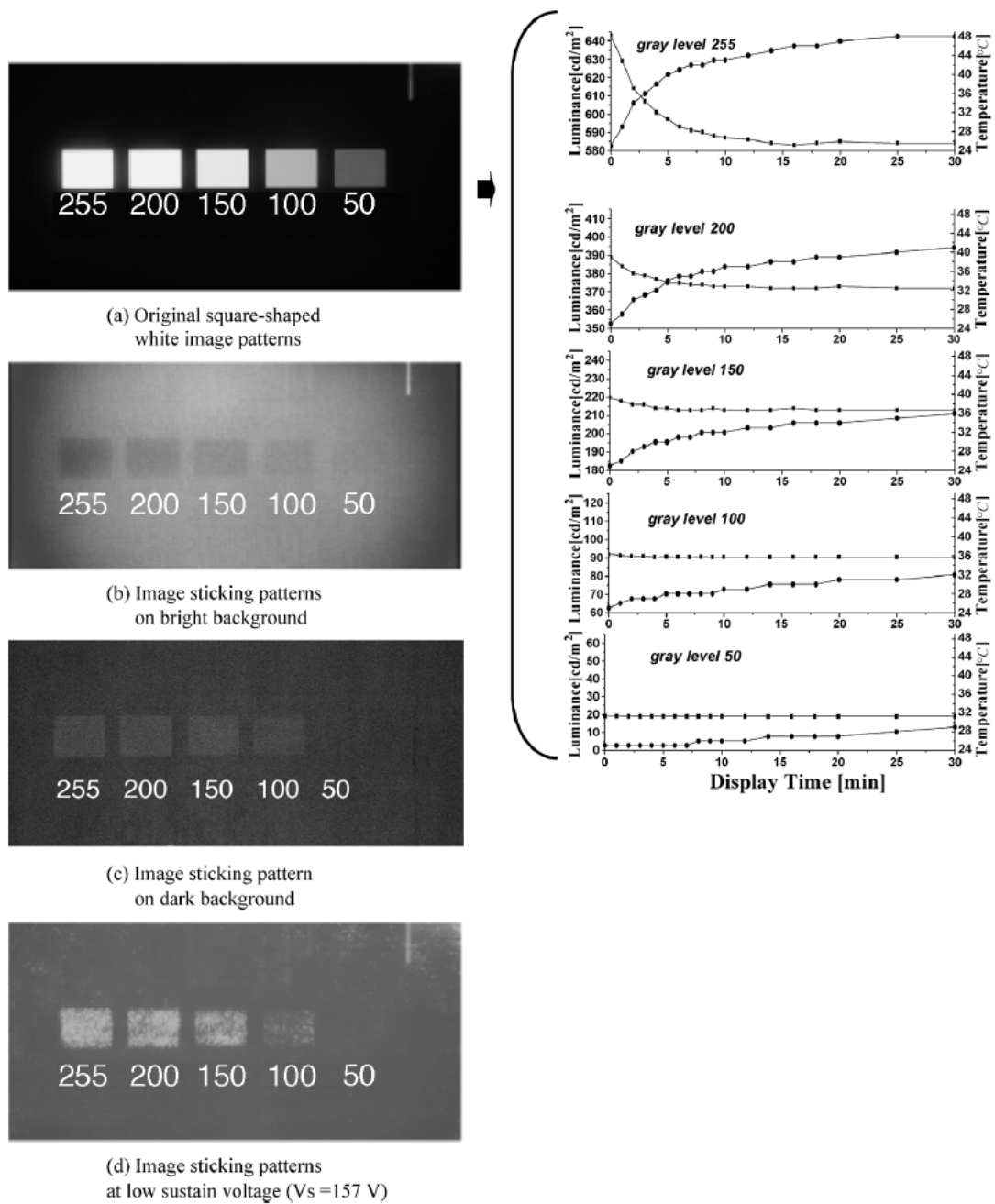


Fig. 3.5 (a) Original square-shaped white image patterns displayed for 15 min at sustain voltage of 176 V, and luminance degradation and rise in cell temperature with variations in gray levels from 50 to 255 during 30-min sustain discharge, (b) image sticking patterns on bright background, (c) image sticking patterns on dark background, and (d) image sticking patterns at low-sustain voltage (= 157 V). [4]

Fig. 3.6 (a) shows the changes in the IR (828 nm) waveforms emitted from the discharge cells (*i.e.*, image sticking cells) during a ramp-up period and the cell temperature rise when the white image pattern is displayed for 60 min. Here, the cell temperature is assumed to be the temperature measured on the front glass. As shown in Fig. 3.6 (a), the IR peak was shifted to the left direction, indicating that the weak reset discharge was initiated efficiently at a lower starting discharge voltage during a ramp-up period. Furthermore, the IR emission was broadened, implying that the reset discharge was produced more efficiently due to the activation of the MgO surface caused by the cell temperature rise. The variations in the IR waveform show the gradual saturation characteristics as the cell temperature was increased due to an iterant strong sustain discharge. Fig. 3.6 (b) shows the recovery characteristics of the IR waveform in the discharge cells when only the reset discharge is produced after the iterant strong sustain discharge. As shown in the IR recovery characteristics of Fig. 3.6 (b), it was observed that the IR emission characteristics were returned to the initial state as the cell temperature was recovered to the initial temperature.

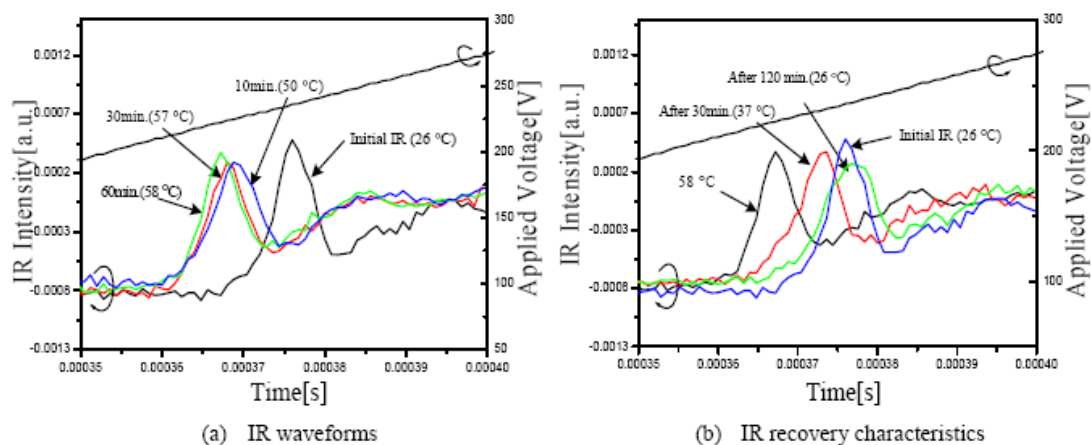


Fig. 3.6 (a) IR waveforms emitted from discharge cells including cell temperature rise under white image pattern during ramp reset-period as function of display time and (b) IR recovery characteristics. [6]

Fig. 3.7 (a) shows the changes in the IR (828 nm) waveforms emitted from the cells adjacent to the discharge cells (*i.e.*, image sticking cells) during a ramp-up period and the cell temperature rise when the white image pattern is displayed for 60 min. As shown in Fig. 3.7 (a), the cell temperature rose even in the adjacent cells, even though the cell temperature of the adjacent cells was slightly lower than that of the discharge cells. The cell temperature rise in the adjacent cells is due to the cell temperature rise in the discharge cells, even though the discharge was not produce in the adjacent cells. The resultant IR peak of the adjacent cells was shifted to the left direction due to the cell temperature rise, which is very similar to the result of Fig. 3.6 (a). The result of Fig. 3.7 (a) means that even in the adjacent cells, the weak reset discharge was efficiently initiated at a lower starting discharge voltage during a ramp-up period.

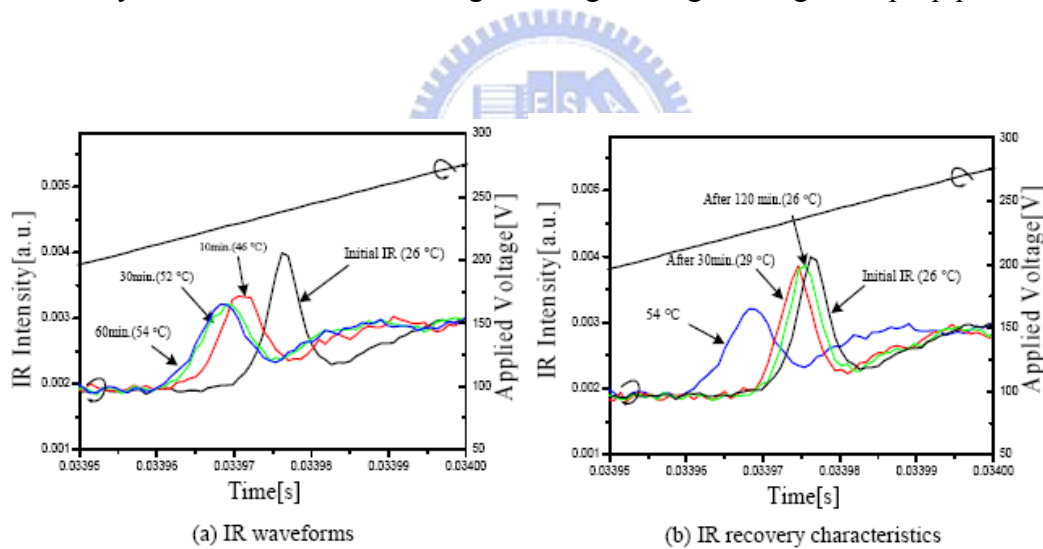


Fig. 3.7 (a) Changes in IR waveforms emitted from cells adjacent discharge cells including cell temperature under white image pattern during ramp reset-period as function of display time, and (b) IR recovery characteristics. [6]

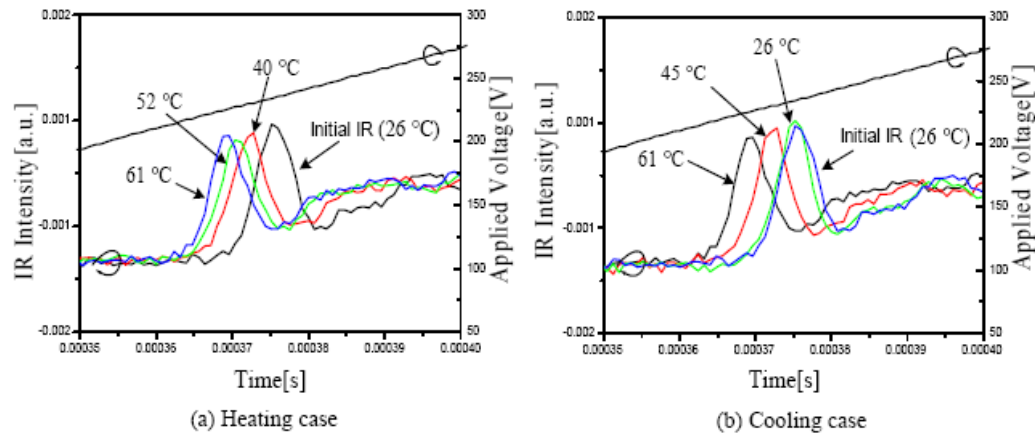


Fig. 3.8 Changes in IR waveforms emitted from cells during ramp reset-period when the front panel is heated by heater at various temperatures. [6]

Fig. 3.7 (b) shows the recovery characteristics of the IR waveform in the adjacent cells when only the reset discharge is produced after the iterant strong sustain discharge. The recovery characteristics of the adjacent cells showed the same tendency as that of the discharged cells of Fig. 3.6 (b). Fig. 3.8 (a) shows the changes in the IR waveforms emitted from the cells during a ramp reset-period when the front panel is heated by the external heater at various temperatures ranging from 26 °C to 61 °C. Fig. 3.8 (b) shows the IR recovery characteristics during a ramp reset-period when the front panel is cooled from 61 °C to 26 °C. As shown in Fig. 3.8 (a), the IR peak was shifted to the left direction, which implied that the breakdown voltage could be decreased simply by increasing the cell temperature without producing the discharge. This phenomenon is the almost same as that of Figs. 3.6 (a) and 3.7 (a). As such, it is concluded that once the cell temperature rises due to either the iterant strong sustain discharge or the heating by the external heater, the corresponding breakdown voltage is decreased. The lower breakdown voltage causes the increase in the IR emission during the reset-period, thereby resulting in a temporal dark image sticking phenomenon in either the discharge cell or adjacent cells. By the way, under the dark background image, the luminance of the adjacent cells (*i.e.*, boundary image sticking

cells) was observed to be higher than that of the discharge cells (*i.e.*, image sticking cells). This phenomenon can be explained as follows: in the discharge cells, the iterant strong sustain discharge causes a deterioration of the phosphor layers, implying that the luminance characteristics is degraded in the discharge cells, whereas the phosphor layer is not degraded in the adjacent cells because of no discharge.

3.1.3 New Driving Method to Reduce Background TIS

From the results of light waveform measurement, Ho-Jun Lee suggest that excessive accumulation of positive charge on the address electrode may cause over discharge and be a source of background ITS. Based on this assumption, they devised a modified driving procedure. During the sustaining discharge, pulse of small amplitude is applied to data electrodes at the end of each sustain period as shown in Fig. 3.9. This positive pulse can clear the wall charges by attracting electron or repulsing positive ions at the afterglow period. Therefore the possible reason for lower firing voltage may be eliminated and BIS phenomenon may be suppressed.

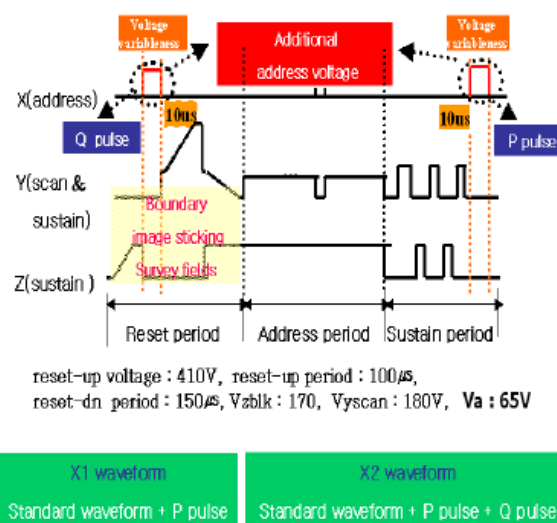


Fig. 3.9 New driving method for reducing background ITS [5]

The amplitude and width of the positive pulse are 10 V and 10 μ sec. Fig. 3.10 shows background luminance of turn-off cells. The suggested method exhibits improved characteristics. However the improvement is not so dramatic because the pulse can control only small amount of charges in afterglow stage

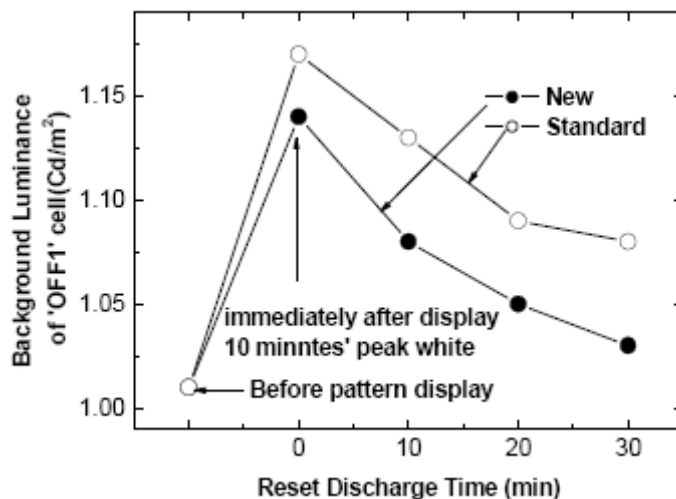


Fig. 3.10 Background luminance of OFF1 cells for proposed and conventional driving method [5]

3.1.4 Summary

Experimental analysis for temporal image sticking has been performed.

1) An iterant strong sustain discharge over a few minutes causes an image sticking problem.

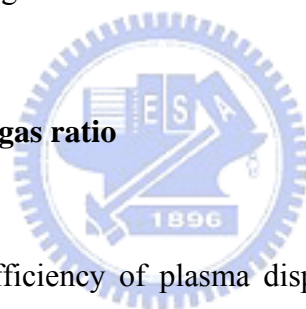
2) When the subsequent image is dark, image sticking makes a brighter ghost image than the background. The outer boundary of patterned area shows highest luminance.

The temperature rising significantly results in faster IR emission and lower firing voltage in the discharged cell and adjacent cell (even though this region is non-discharge region). In this case, since the luminance of the dark image is only produced by the weak reset discharge, the higher luminance of the ghost image is

mainly due to the activation of the MgO surface. Excessive wall charge accumulation and alteration of MgO surfaces due to transport of neutral particles are thought to be one of the main sources of boundary background TIS. It has been demonstrated that positive pulse applied on the data electrode mitigate the boundary background TIS[5]. However, the new driving method to clear the excessive accumulated wall charge does not improve BIS dramatically.

3) Conversely, when the subsequent image is bright, image sticking makes a darker ghost image than the background. The experiment proves that lower luminance of the ghost image is mainly due to the temporal degradation of the phosphor layer caused by the temperature arising. No matter for WIS or BIS, the luminance difference could recover when the temperature gets back to lower value.

3.2 Influence of Xe-Ne inert gas ratio



At present-day the light efficiency of plasma display panel, typically about 1~2 lm/W, is rather low in comparison with CRT about 5 lm/W. Thus efficiency improvement is a major objective in plasma display research. As Chapter 2 mentioned, the efficacy of an alternating current surface-discharge plasma display can be divided into contributions from successive conversion factors: vacuum-ultraviolet (VUV)-generation, VUV capture by a phosphor coating, VUV to visible light conversion, and visible light losses. The discharge is a predominant factor limiting the overall efficiency. For default NeXe gas mixtures containing about 5% Xe the discharge efficiency is typically 10%. It is well established that the discharge is strongly influenced by the gas mixture composition, especially the Xe partial pressure. In this section, the research about Ne-Xe gas mixture in AC-PDP is discussed.

Fig 3.11 and 3.12 show the dependence of luminous efficiency, firing voltage (V_f) and minimum sustaining voltage (V_{sm}) for Xe content of several test panels. These results indicated that higher Xe content gas would increase the VUV and visible light generation with the increase of firing voltage.

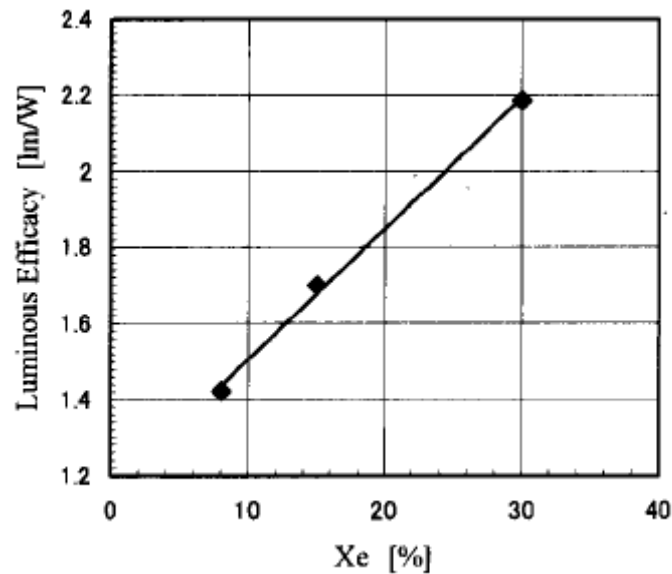


Fig 3.11 Dependence of luminous efficiency for several Xe partial pressures (Total pressure: 667hPa) [7]

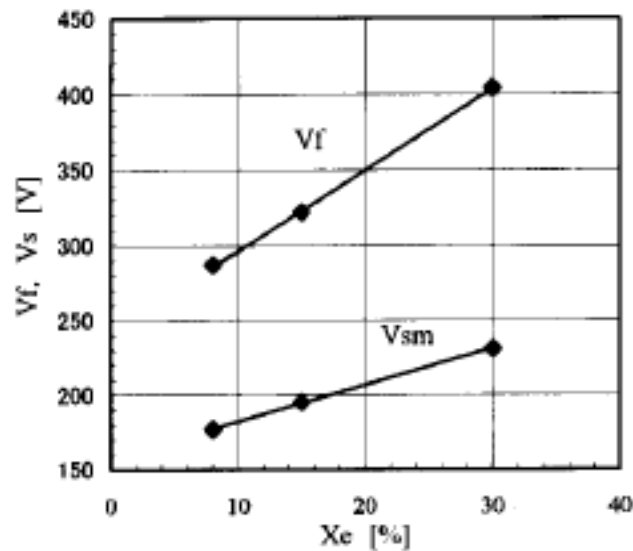


Fig 3.12 Dependence of firing voltage (V_f) and minimum sustaining voltage (V_{sm}) for several Xe partial pressures (Total pressure: 667hPa) [7]

A higher Xe content gas causes instability of selecting discharge. To avoid this problem, the addressing voltage should be increased, but it causes another problem to the driving circuit.

It is concluded that the discharge efficiency for the cell geometry used in present-day commercial products can be increased significantly by using a larger Xe partial pressure, at the cost of a moderate increase of the operation voltages. Furthermore, panel chromaticity improves for higher Xe partial pressure. An increase of the electron heating efficiency and of the Xe excitation efficiency both contribute about equally to the efficacy increase for increasing Xe partial pressure. The increase of the Xe excitation efficiency is due to an increase of the excitation in the lower Xe levels induced by a lowering of the electron temperature. The increase of the electron heating efficiency is tentatively attributed to an increasing ionization at lower potential energy in the cathode sheath region. It is further noted that a higher panel efficacy does not necessarily imply a higher system efficiency. A higher Xe partial pressure causes higher discharge voltages, which in turn lead to higher losses in the electronic system. Also, the high voltage driving results in high cost electronic circuit.

3.3 MgO and Phosphor Doping and Contamination

The degradation of the MgO protective layer and the phosphorous layer plays a very important role for the PDP lifetime performance because both layers are exposed to plasma in the cell. In this section, information about degradation of the MgO layer and the phosphorous layer for AC-PDP is discussed.

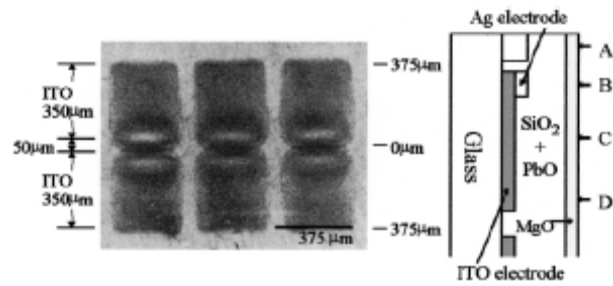


Fig. 3.13 SEM images of the AC-PDP micro cell structure [8]

Fig. 3.13 shows the low magnification SEM image of the AC-PDP after the 1000-h operation with the schematics of the micro-cell structure. The spatial variation in the contrast reveals that the erosion of the MgO layer was not uniform; note the signature of more severe erosion near the edges of the ITO electrodes. The non-uniform erosion of the MgO layer was more clearly demonstrated by the high magnification SEM images shown in Fig. 3.14 In this figure, SEM pictures were taken at four different positions in a single micro-cell, which corresponded to the black strip A., the Ag electrode B, the middle of the ITO electrode C, and the edge of the ITO electrode D, respectively. (see Fig. 3.13) The position A was immune to the ion bombardment, and consequently, the surface texture of the MgO layer remained intact. However, other positions experienced ion bombardment, which resulted in the leveling of the MgO-surface texture by removing the local asperity and filling in the grain boundaries. Note that the leveling of the MgO surface was more pronounced near the ITO sustaining electrode edge (position D).

The operation-time-dependent erosion of the MgO layer from the SEM images was presented in Fig. 3.15 These SEM pictures correspond to the position C of a virgin AC-PDP and those of two other ones operated at the sustaining voltage of 180 V for 9 and 1000 h, respectively. It was interesting to note that the leveling of the MgO-surface texture, which was already noticeable after only the 9-h operation, was

so significant after the 1000-h operation that individual MgO crystallite were completely indiscernible even at the middle of the ITO electrode.

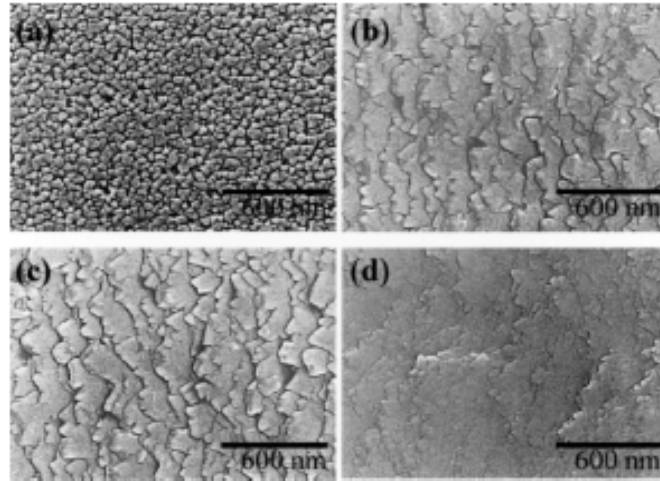
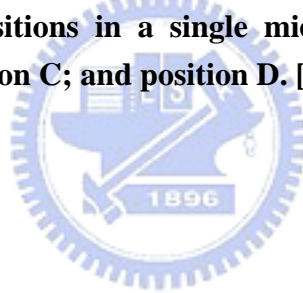


Fig. 3.14 Spatial variation of the MgO surface in the a.c.-PDP. SEM pictures were taken at the four positions in a single micro-cell marked in Fig. 3.13: position A; position B; position C; and position D. [8]



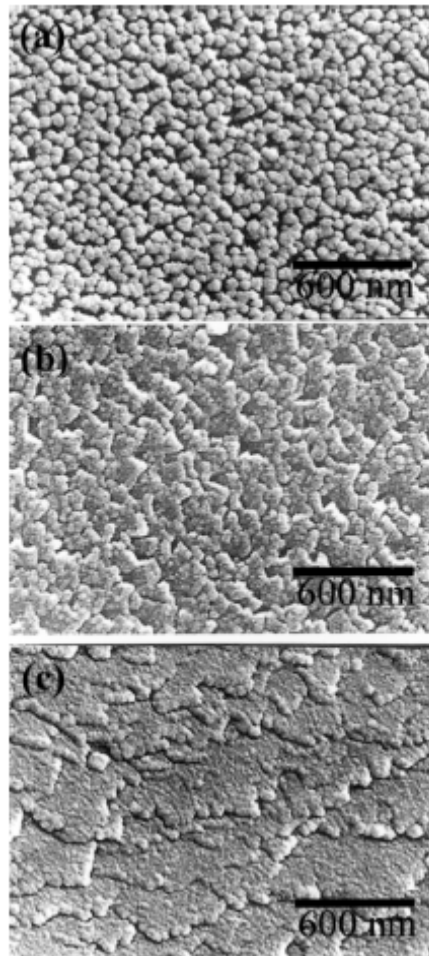


Fig. 3.15 SEM images of a virgin a.c.-PDP and two other ones operated at the sustaining voltage of 180 V for 9 and 1000 h, respectively. All three pictures correspond to the position C (see Fig. 3.13) [8]

More dramatic evidence for the non-uniform erosion of the MgO layer came from the surface profiler. Fig. 3.16 shows a series of 3-dimensional surface profiles of the MgO-layer in a single PDP-cell operated at 180 V and 10 kHz. The presented profiles were produced assuming that the surface of the virgin cell was flat. The surface profiles show that the two main features of the MgO-layer alteration were the formation of two trenches near the ITO-electrode edges due to the erosion and the thickening of the MgO-layer in the mid-region between two ITO electrodes due to the re-deposition of eroded MgO. Moreover, the surface profiles show that the erosion and the re-deposition occurred nearly uniformly along the y direction of ITO as

expected from the construction of a PDP-cell. Temporal progress of the erosion and the re-deposition can be examined in detail from the normalized-thickness curves presented in Fig. 3.17. The lateral position represents the position in the direction perpendicular to the ITO electrode (x direction in Fig. 3.13).

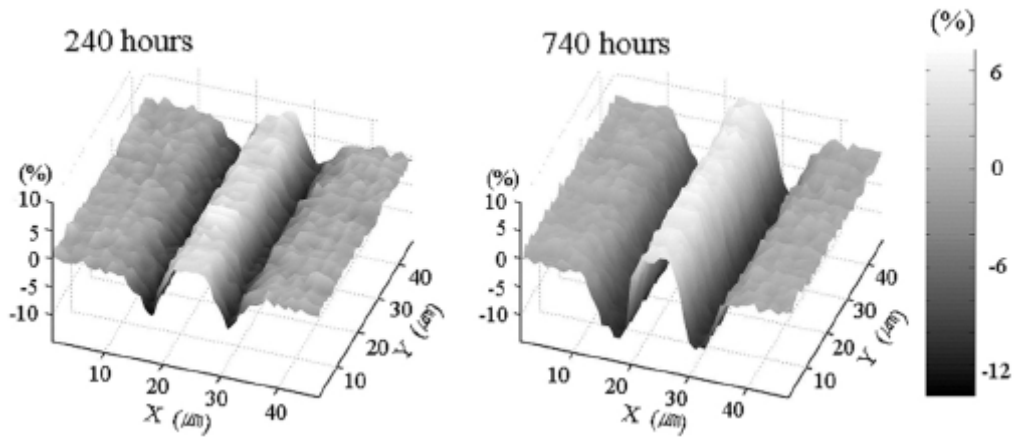


Fig. 3.16 3-Dimensional surface profiles of the MgO-layer in a PDP-cell

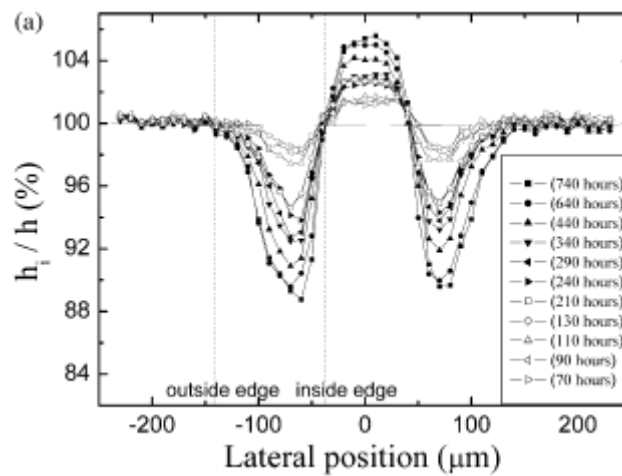


Fig. 3.17 The normalized-thickness curves vs. lateral position [9]

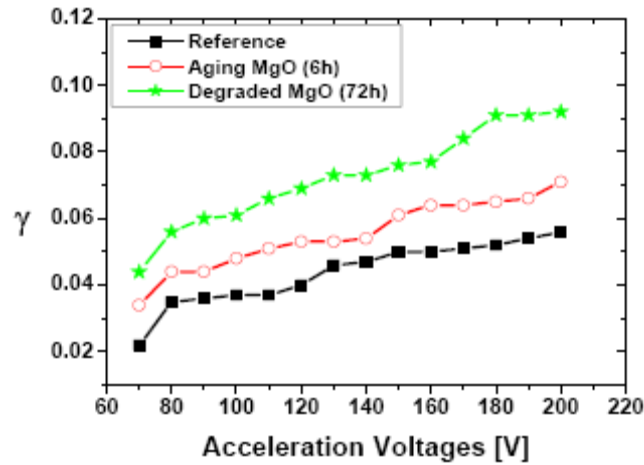


Fig 3.18 Secondary electron emission coefficient (γ) of MgO thin films with different degraded condition [10]

In Jeong Eun Lim’s work, the PDP was divided into three parts; one experienced aging for 6 h, another one is degraded for another 72 h and the last one is reference. They found the secondary electron emission coefficient (SEEC, γ) of the MgO increases with degraded time, as Fig. 3.18 shows.

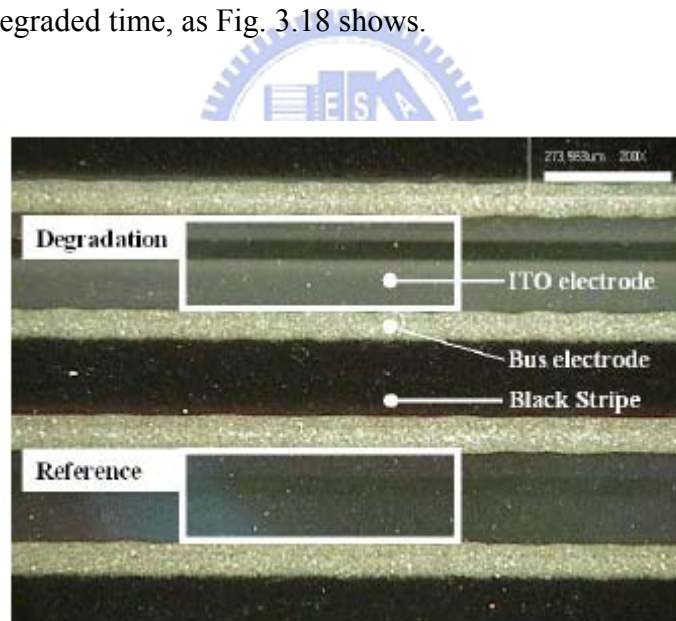


Fig. 3.19 Change of MgO protective layer before and after discharge [10]

Figure 3.19 shows change of MgO protective layer before and after degradation, which is magnified 200X. It is found that MgO protective layer becomes rather opaque than that before degradation and then the luminance of AC-PDP has been influenced by it. Actually, luminance of test panel after degradation is decreased

about 25 cd/m². Even though the firing voltage decreases due to the increase of secondary electron emission coefficient, the luminance decrease resulted from the degraded phosphor or MgO thin films with low transparency.

In recent years, the phosphor is greatly improved. Right now the most widely used phosphors for PDP application is (Y,Gd,Eu)BO₃, (Zn,Mn)₂SiO₄, (Ba,Eu)MgAl₁₀O₁₇ for Red, green and blue, respectively. Table 3.1 shows the specific data of the phosphors.

Color	Composition	Color coordinate x	Color coordinate y
Blue	(Ba,Eu)MgAl ₁₀ O ₁₇	0.146	0.067
Green	(Zn,Mn) ₂ SiO ₄	0.244	0.702
	Ba,Sr,Mg)O. aAl ₂ O ₃ : Mn	0.145	0.747
	(Y,Gd,Tb)BO ₃	0.321	0.61
Red	(Y,Gd,Eu)BO ₃	0.641	0.356
	(Y,Gd,Eu) ₂ BO ₃	0.642	0.344
	(Y,Eu)(PV)O ₄	0.657	0.333

Tab. 3.1 The specific data of the phosphors

For the red, green and blue phosphors for PDP, the blue one has the shortest lifetime. Thus, it is essential to improve the lifetime of the blue phosphor. However, due to the crystal structure of the BAM, it is not easy to improve its lifetime. The new phosphor CaMgSiO₆:Eu(CMS) and 1.3BaO·6Al₂O₃ with new structure is under development. These two new materials have lower luminous efficiency but longer lifetime than those of BAM. The recent research revealed that addition of Cd into CMS results in higher luminous efficiency.

The green phosphor, $(\text{Zn,Mn})_2\text{SiO}_4$ has the highest luminous efficiency but longer decay time compared with the other two. It is widely used in PDP TV and CRT TV. The electrical properties of $(\text{Zn,Mn})_2\text{SiO}_4$ is different with the red and blue phosphor. For instance, when we use $(\text{Y,Gd,Eu})\text{BO}_3$ as red, $(\text{Y,Gd})\text{BO}_3$ as green, BAM as blue phosphor, only address voltages of green cells increase. Coating on the surface of $(\text{Zn,Mn})_2\text{SiO}_4$ can improve the electrical characteristic.

$(\text{Y,Gd,Tb})\text{BO}_3$ is a new phosphor material having similar structure with red phosphor $(\text{Y,Gd,Eu})\text{BO}_3$. Its electric characteristic is also similar with $(\text{Y,Gd,Eu})\text{BO}_3$. When we combine $(\text{Y,Gd,Tb})\text{BO}_3$ and P1-G1S, the better electric characteristic and long lifetime are achieved. However, $(\text{Y,Gd,Tb})\text{BO}_3$ has little worse color purity than the other. $(\text{Y,Gd,Eu})\text{BO}_3$ is the only practical red phosphor with high luminance and long lifetime. Its disadvantage is bad color purity and long decay time. To improve color purity, it is essential to use front filter to remove some emission light. $(\text{Y,Gd,Eu})_2\text{BO}_3$ and $(\text{Y,Eu})(\text{PV})\text{O}_4$ have good color purity and 70% luminance of the KX-504A. Its lifetime is almost the same as the KX-504A.

Chapter 4 Investigation Method and Experimental Setup

In chapter 3, recent researches about erosion of the Magnesium Oxide (MgO) and phosphors have been reviewed. The influence of noble gas mixture on AC-PDP is discussed. Besides, the image sticking phenomenon is introduced. The motivation, investigation method and experimental setup of this work are described.

4.1 Motivation and Investigation Method

This research will focus on two major aspects. One is the degradation and contaminations of the MgO thin films caused by phosphors. The other is the influence of the noble gas mixture on the image sticking phenomenon.

As mentioned in chapter 3, MgO thin films and phosphors play a very important role for the AC-PDP panel performance because both layers are exposed to plasma in the cell [24, 26]. The variation of secondary electron emission coefficient (SEEC) and ability of accumulating wall charge on the surface also change the minimum and maximum sustain voltage of AC-PDP. The luminance efficiency of PDP is reduced due to the decreasing transparency of MgO thin films because of ion bombardment and contaminants. The degradation of phosphorous layer also leads to decreased luminance and the worse color performances in PDPs [19, 22, 23, 25].

Even though the MgO thin films and phosphorous layers have great influence for the panel, there is currently no report of the degradation of MgO thin films by the phosphorous layer in AC-PDP as a whole. Therefore, we propose to figure out which properties of MgO thin films has the largest influence on the panel properties. The result will be discussed in 5.1 and 5.2.

For image sticking phenomenon, the TIS has been related to the activation of MgO surface or the degradation of phosphor layers during the strong sustained discharges [4,5,6,7]. Recently, PDP manufacturers and research groups are concerning about high Xe panel for efficiency improvements. In a conventional Ne-Xe gas mixture, it is well known that the increase of Xe contents results in the increases of luminance and luminous efficiency while it also results in the increase of the breakdown voltage and the discharge time lag [7, 15, 16]. For higher luminous efficiency, it may generate less heat in the discharge cells. Thus the temperature may decrease and the degree of white image sticking phenomenon may be suppressed. For higher breakdown voltage, the miss discharge may decrease and background image sticking could be suppressed, too.

The purpose of this paper is analyzing the degree of temporal image sticking and to find the influence of the gas concentration on the image sticking phenomenon. The image sticking phenomena are observed with white patterns in the work. For R, G, and B cells, the changes in the luminance with time are discussed. In the 5.3, the relational result will be presented.

4.2 Measurement System

Forty-six inch WVGA panels were made for this work. The PDP panels are powered by the power system GPS06CM. The color coordinates, color temperature and luminance are measured by color analyzer CA-100. Voltage and light signals are measured by a digital oscilloscope with photo receiver connected. The image patterns are generated from the pattern generator. Fig. 4.1 shows the whole measurement system.

One of the experimental PDP module is shown in Fig. 4.1. The MgO films were deposited on the PDP's front panel by electron beam evaporation. Also, the conventional phosphorous layers of PDPs were printed on the rear panels: the main component of red, green and blue phosphorous layers are (Y, Gd, Eu) BO₄, (Zn, Mn)₂SiO₄ and (Ba, Eu) MgAl₁₀O₁₇, respectively. Panels are fabricated with Neon and Xe inert gas. Some panels are varied with Xe partial pressure and total gas pressure. In this paper, an accelerated relative-lifetime-test for MgO thin films is proposed by using higher operating voltage and sustained frequency than those of normal conditions. After operating for a period of time, panels were investigated to identify the surface morphology and contaminations of MgO thin films using Atomic Force Microscopy (AFM), X-ray Photoelectron Spectroscopy (XPS) as Fig. 4.2 shows.

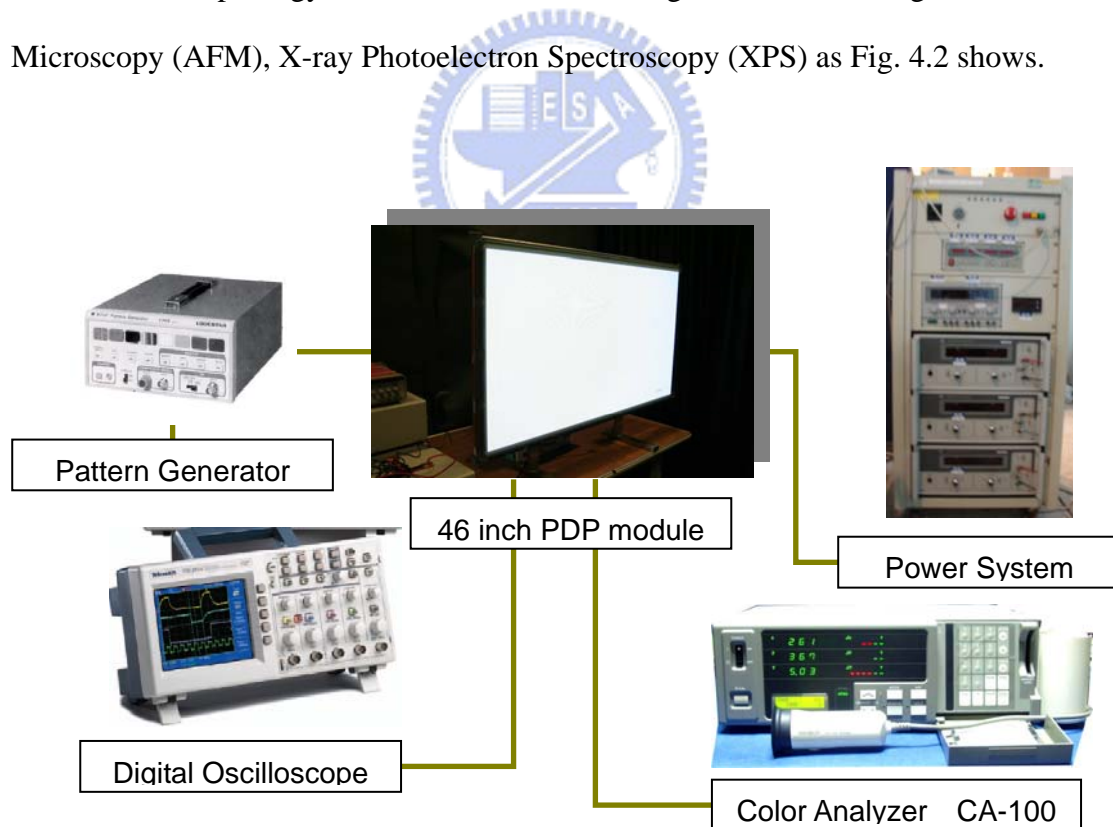


Fig. 4.1 Electrical and optical measurement system



Fig. 4.2 X-ray Photoelectron Spectroscopy (XPS), VG Scientific, Microlab 350



Chapter 5 Results and Discussion

5.1 Variation of Driving Margin

In this work, full sized forty-six inch panels were made. The MgO films were deposited on the PDP's front panel by electron beam evaporation. Also, the conventional phosphorous layers for PDP application were printed on the rear panels. In order to figure out the relationship between phosphor and MgO thin films, some experimental panels are made with mono color, which means only one phosphor is printed on the panel. As Tab. 5.1 shows, the panel No.1 and No. 2 are printed with red phosphor. Panel No.3 and No.4 are printed with green phosphor. Panel No. 5 and No. 6 are printed with blue phosphor. Panel No. 7 and No. 8, as conventional PDP panels, are printed with red, green and blue phosphor. The main component of red, green and blue phosphorous layers are $(Y, Gd, Eu) BO_4$, $(Zn, Mn)_2SiO_4$ and $(Ba, Eu) MgAl_{10}O_{17}$, respectively. Each color is provided by two companies. KX504A, P1G1S are manufactured by KASEI OPTONIX. NP360-53, NP200-205 and NP107-743 are manufactured by NICHIA co. One of the blue phosphor is made by LG Chem.

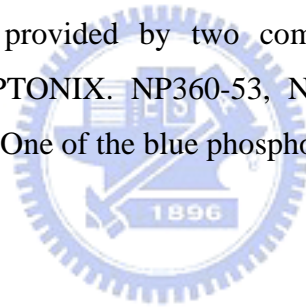


Table 5.1 Experimental PDP Setup

Panel No.	Phosphor Name	Main Component	Abbreviated Name	Manufacturer
1	KX-504A	(Y,Gd,Eu)BO ₃	YGB	KASEI OPTONIX
2	NP360-53	(Y,Gd,Eu)BO ₃	YGB	NICHIA co
3	P1-G1S	(Zn,Mn) ₂ SiO ₄	ZSM	KASEI OPTONIX
4	NP200-205	(Zn,Mn) ₂ SiO ₄	ZSM	NICHIA co
5	NP107-743	(Ba,Eu)MgAl ₁₀ O ₁₇	BAM	KASEI OPTONIX
6	LG Chem	(Ba,Eu)MgAl ₁₀ O ₁₇	BAM	LG Chem
7	R:NP360-53 G:NP200-205 B: LG Chem	(Y,Gd,Eu)BO ₃ (Zn,Mn) ₂ SiO ₄ (Ba,Eu)MgAl ₁₀ O ₁₇	YGB ZSM BAM	
8	R:KX-504A G:P1-G1S B:NP107-743	(Y,Gd,Eu)BO ₃ (Zn,Mn) ₂ SiO ₄ (Ba,Eu)MgAl ₁₀ O ₁₇	YGB ZSM BAM	

To speed up the degradation of MgO thin films and phosphorous layer, the experimental panels were sent into the aging process. The process what we called aging plays a very important role for PDP panels. For typical ac-PDP manufacture process, the panels are sent into aging for several hours after fabrication. During aging, high-frequency sustained pulse is applied to the panels. For mass production line, the purpose of this process is to activate the MgO thin films and make the panel performance stable. Aging process is time consuming but essential for high-quality panels. For typical ac-PDP, aging lasts for only 18 hours. In this work, the experimental panels are sent into aging for 1000 hours to achieve faster degradation. Luminance, color performance and driving margin are recorded at the selected time to observe the variation of panel properties.

Before we continue, one of the measurement techniques called dynamic driving margin should be introduced first. The margin area defines the range of applied

voltage. The V_s indicated the sustain voltage while V_{xg} represents the address voltage. For PDP driving, both the applied V_s and V_{xg} must be in the margin area otherwise the ow or iw occurs in some areas on the PDP panels. Ow, which means over write, usually occurs when too high voltage is applied to the panels. Luminance in the ow cells appear to be higher than the normal cells. Sometimes cross talk with other sub cells appears simultaneously and makes luminance and color non-uniform for the whole panel. Iw, which means insufficient write, usually occurs when too low voltage is applied on the panel. Luminance in the iw cells is lower than other cells. The cells can not be ignited completely so the flicker occurs. Lower minimum address and sustain voltage can decrease power consumption and cost of driving circuit. The variation of margin data as a function of time could be observed. Fig. 5.1 (a) and (b) show the driving margin area of the No.1 panel after accelerated test time 18 hour and 1000 hour, respectively.

After long time operation, the minimum address voltage increased, while minimum sustain voltage decreased. The maximum address and sustain voltage decreased and made the driving margin area decrease. This is due to the degradation of MgO thin film by the ion bombardment in plasma. Fig. 5.2 to Fig. 5.8 shows the variation of driving margin of panel No.2 to No.8. From the result, the panels with red phosphor have an obvious degradation. However, the Panels with green phosphor only varied slightly. The panels with blue phosphor almost remain the same. The panels with three kinds of phosphor (red, green and blue phosphor) also have obvious degradation. The driving margin is directly related to properties of MgO thin films. In this experiment, MgO thin films of all panels are deposited with the same parameters by one machine. The only difference is their phosphor. Therefore, we demonstrated that the degraded margin area of the panel No. 1 and No.2 is caused by contaminations in the Mgo thin films by red phosphor. We think red phosphor also cause the degradation of panel No.7 and No.8.

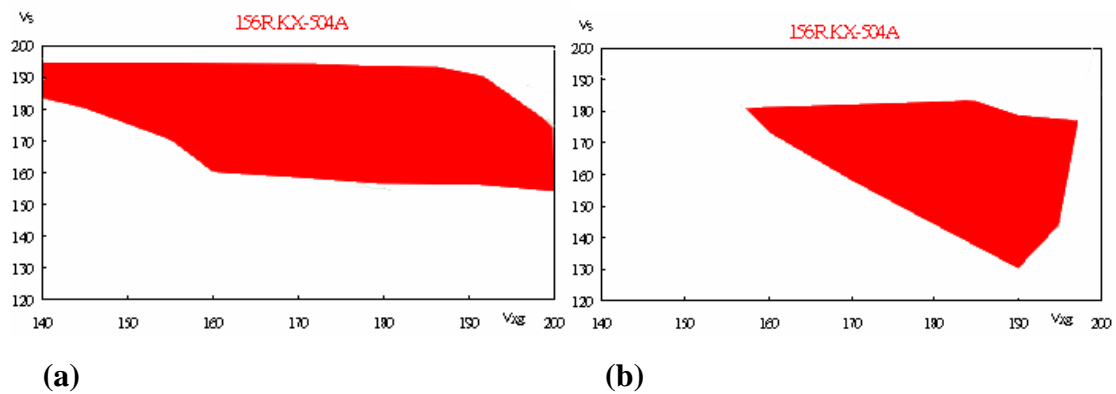


Fig 5.1 The driving margin of the panel with red phosphor KX504A after (a) 18 hour and (b) 1000 hour accelerated test time (aging).

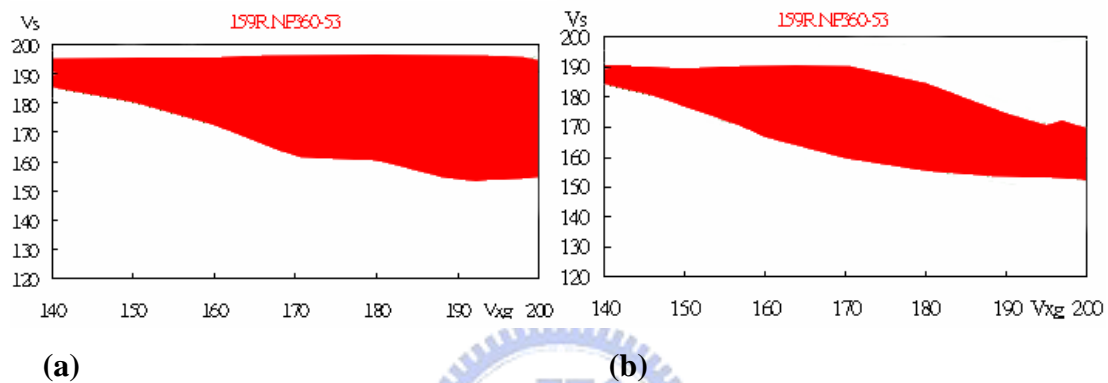


Fig 5.2 The driving margin of the panel with red phosphor NP360-53 after (a) 18 hour and (b) 1000 hour accelerated test time (aging).

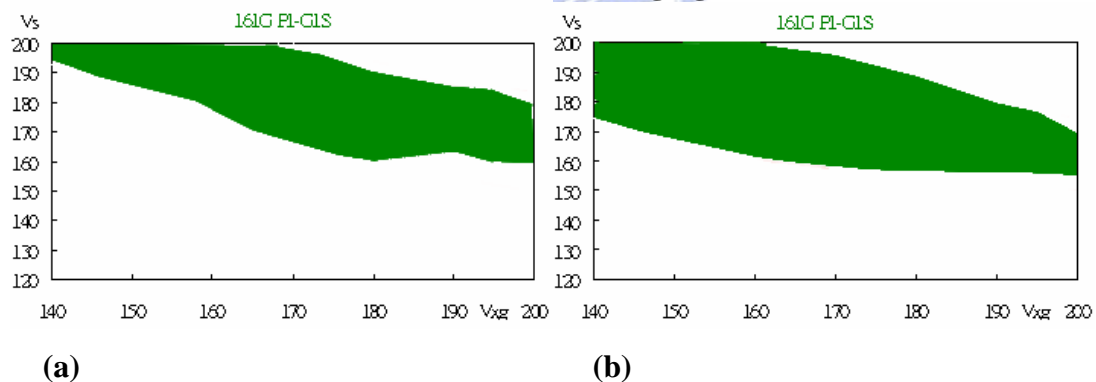


Fig 5.3 The driving margin of the panel with green phosphor P1G1S after (a) 18 hour and (b) 1000 hour accelerated test time (aging).

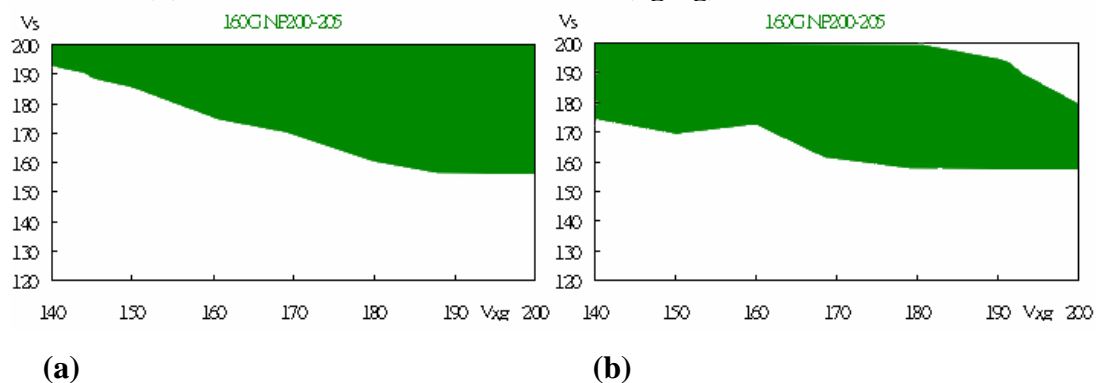


Fig 5.4 The driving margin of the panel with green phosphor NP200-205 after (a) 18 hour and (b) 1000 hour accelerated test time (aging).

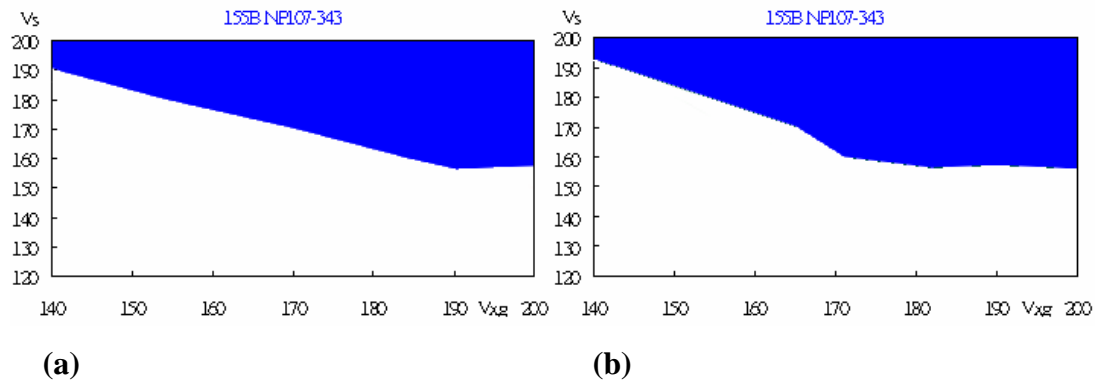


Fig 5.5 The driving margin of the panel with blue phosphor NP107-343 after (a) 18 hour and (b) 1000 hour accelerated test time (aging).

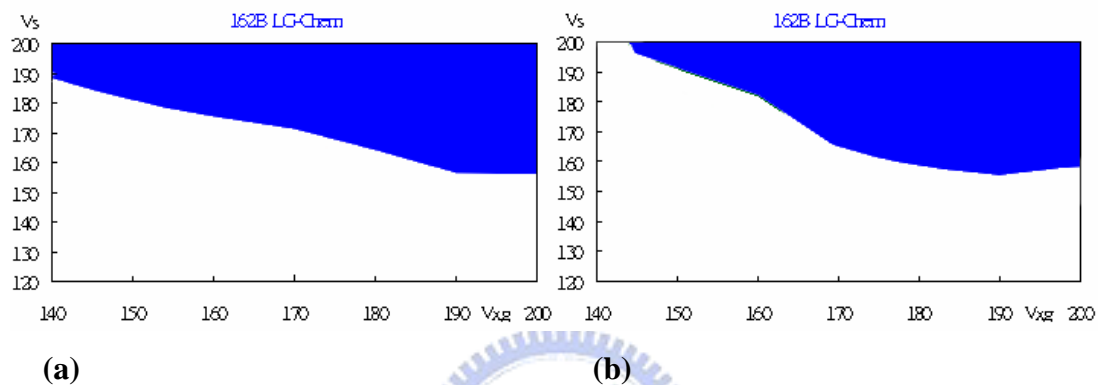


Fig 5.6 The driving margin of the panel with blue phosphor LG Chem after (a) 18 hour and (b) 1000 hour accelerated test time (aging).

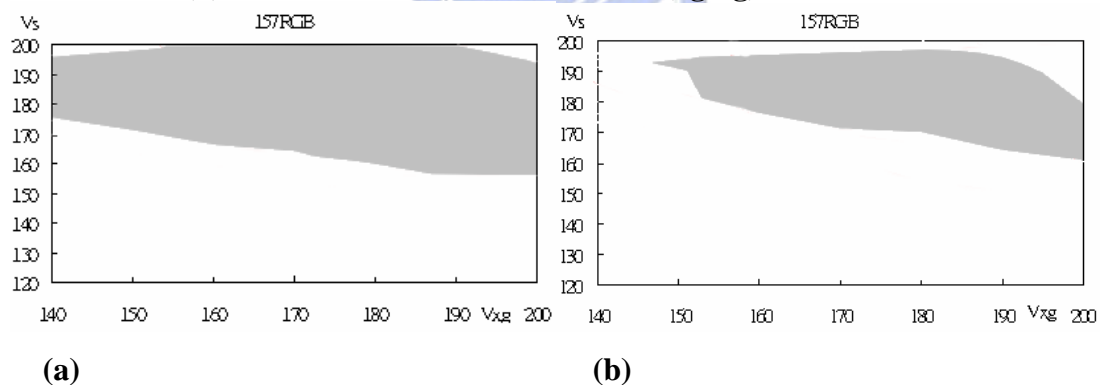


Fig 5.7 The driving margin of the panel with RGB phosphor after (a) 18 hour and (b) 1000 hour accelerated test time (aging).

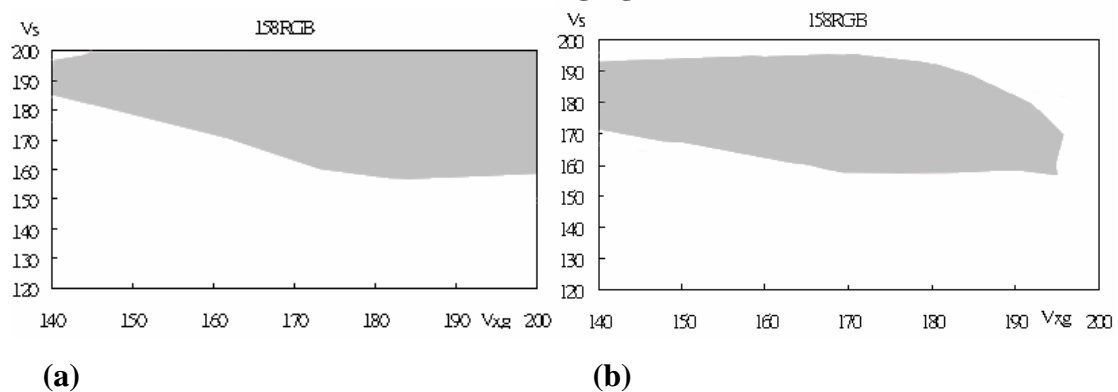


Fig 5.8 The driving margin of the panel with RGB phosphor after (a) 18 hour and (b) 1000 hour accelerated test time (aging).

5.2 Contamination of MgO thin films by Phosphors in AC-PDP

In previous section, we demonstrate that red phosphor causes degradation of MgO thin films. In this section, another life time test is performed and the contamination of MgO thin films is investigated.

5.2.1 Experiments

There were two full sized 46-inch panels selected for this experiment. The MgO films were deposited on the PDP's front panel by electron beam evaporation. Again, the conventional phosphorous layers of PDPs were printed on the rear panels: the main component of red, green and blue phosphorous layers are $(Y, Gd, Eu) BO_4$, $(Zn, Mn)_2SiO_4$ and $(Ba, Eu) MgAl_{10}O_{17}$, respectively. The difference between the two panels is the operation mode. To speed up the degradation of MgO protective layer, the PDP No.1 panel was modified as facing sustained mode, which generates plasma vertically between the sustained electrode on the front panel and address electrode on the rear panel, instead of conventional surface type plasma discharge between two sustained electrodes. We have assumed that this setup would make stronger ion bombardment between MgO layer and phosphorous layers, and possibly result in more contamination in the MgO layer caused by phosphors. However, the No.2 panel was operated as a conventional surface discharge type PDP to compare with the No.1 panel. Like previous section, an accelerated relative-lifetime-test for MgO thin films is proposed by using higher operating voltage and sustained frequency than those of normal conditions. After operating for a period of time, panels were investigated to identify the surface morphology and contaminations of MgO thin films using Atomic Force Microscopy (AFM) and X-ray Photoelectron Spectroscopy (XPS).

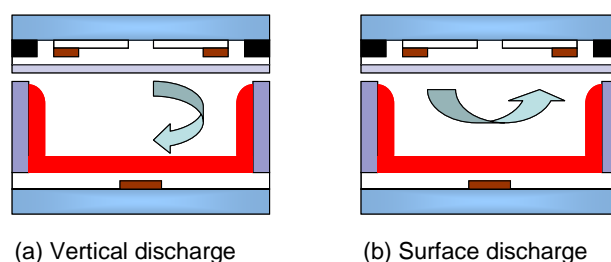
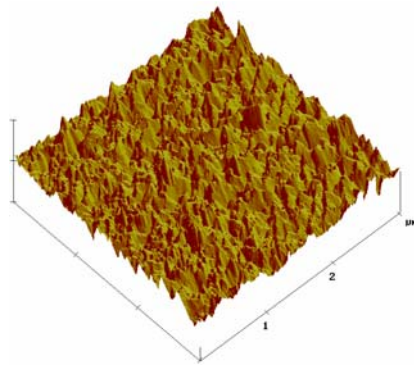


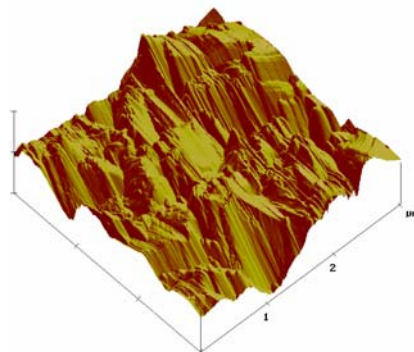
Fig. 5.9 Schematic diagram of the surface sustain discharge and vertical sustain discharge

5.2.2 Results and Discussion

In this work, the 700-hour operation for vertical discharge panel and 16000-hour operation of the surface discharge type panel was performed to degrade the MgO thin film. It is reported that the surface morphology of MgO layer and its degradation is dependent on different areas in a single micro-cell [11]. This makes the surface of the MgO layer non-uniform. Fig. 5.10 shows the surface morphology of the MgO thin film after the accelerated lifetime test by atomic force microscope (AFM). The AFM pictures clearly show evidence of the erosion of the MgO layer. The erosion of the MgO layer in the glow discharge in an ac PDP occurred by ion bombardment on the MgO thin film. After long time sustained discharge, significant grain growth occurred as shown in Fig. 5.10 (a) and 5.10 (b). Especially, the surface profile of the 16000-hour operated sample clearly exhibited that the erosion of the MgO layer was much more severe than the 700-hour one. The RMS roughness of the sample with 16000-hour surface discharge is over 10 times larger than that of the sample with 700-hour vertical discharge. We think that this is because of the much longer time ion bombardment for the surface discharge one. For the same accelerated test time, it is expected that the vertical discharge type panel leads to stronger ion bombardment and changes the surface morphology and thickness of the MgO layer in some specific part.



(a)

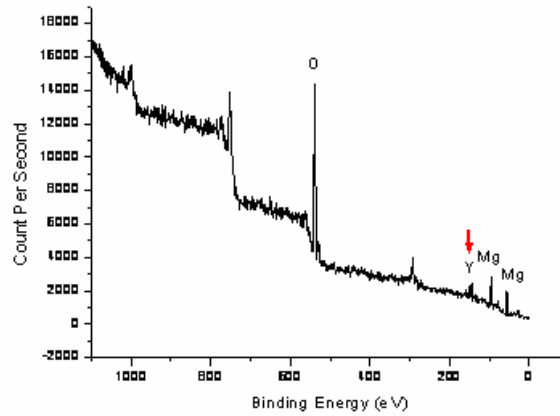


(b)

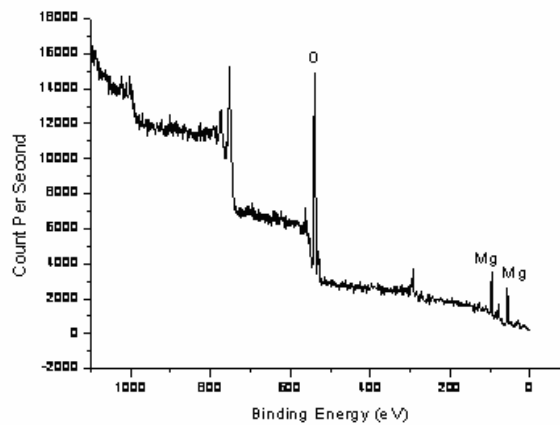
Fig. 5.10 (a) AFM images of MgO thin films vertical discharge type panel after 700-hour accelerated test time. (b) AFM images of surface discharge type panel after 16000-hour accelerated test time.

The XPS analyses are shown in Fig. 5.11 (a) and 5.11 (b) for the vertical discharge type panel and the surface discharge type panel. The figures represent the element in the surface of MgO layer. The peaks for Mg (89 eV) and O (536 eV) can clearly be observed. In Fig 5.11 (a) we also notice the smaller peak around 150 eV, which can be considered as yttrium from the red phosphor (Y, Gd, Eu) BO₄. However, in Fig. 5.11 (b) the yttrium doesn't appear at 150 eV. The elements Fe, Si, Al, and Mn may come from the MgO source material before deposition. However, there is a high possibility that the Yttrium elements come from the red phosphor. The difference between the two panels possibly resulted from the stronger ion bombardments between the MgO layers and the phosphorous layers. The contaminations and ion bombardment may change the surface morphology of MgO thin film. This would affect transparency and the secondary electron emission coefficient related to the luminance and sustained voltage. However, there are no other phosphor elements detected. It may result from different dielectric and surface properties of each phosphor. The green phosphor (Zn, Mn)₂SiO₄ has negative surface discharge while those of red and blue phosphors are

positively charged [12], which results in smaller wall charges stored by the reset discharge in the green cell than in the red or blue cells. This phenomenon would make weaker vertical discharge between the MgO layer and the green cell, which results in little contamination in the MgO thin films.



(a)



(b)

Fig. 5.11 (a) XPS surface analysis of the vertical discharge type panel after 700-hour accelerated test time. (b) XPS surface analysis of the surface discharge type panel after 16000-hour accelerated test time

We think it is difficult to detect the difference for the trace amounts of the impurity and another method needs to be tried.

5.2.3 Summary

In this part, a long-term lifetime test was proposed for MgO thin films in an ac-PDP. The surface morphology and contaminations in the MgO thin films were investigated. By means of XPS, we confirmed that a part of contamination results from ion bombardment to the red phosphors. This result consists with the result shown in previous section. Even though the surface discharge type has stronger erosion on the MgO thin film because of long time discharge, the contaminations for the vertical discharge type were severe. We demonstrated that the degradation of the MgO thin films in AC-PDP was partially caused by contaminations from phosphor. The effect of discharge characteristic changes in the MgO thin films can be an important property which needs to be studied.

5.3 Observation of Image sticking with different Xe partial pressure and total inert gas pressure



5.3.1 Experiments

In this study, the full sized 46-inch panels were made with Xenon (Xe) and Neon (Ne) inert gases. In order to figure out the relationship between the gas concentration and the image sticking phenomena, the Xe gas ratio and total gas pressure are varied at different panels. The Xe gas ratio is set at 6% and 9%, while the total gas pressure is set at 475 torr and 550 torr. Table 1 represents the experiment setup for the whole panels in the work. The conventional ac-PDP has 4%~5% Xe partial pressure and 475 torr total inert gas pressure. So the panel with 6% Xe ratio and 475 torr total pressure is taken as reference panel. For investigation of the image sticking phenomenon, a square pattern with 4% panel surface area and full white 255 gray level is displayed at the center of the panel. For a period of displayed time, the 4% pattern is changed to full white background to observe the white image sticking phenomenon.

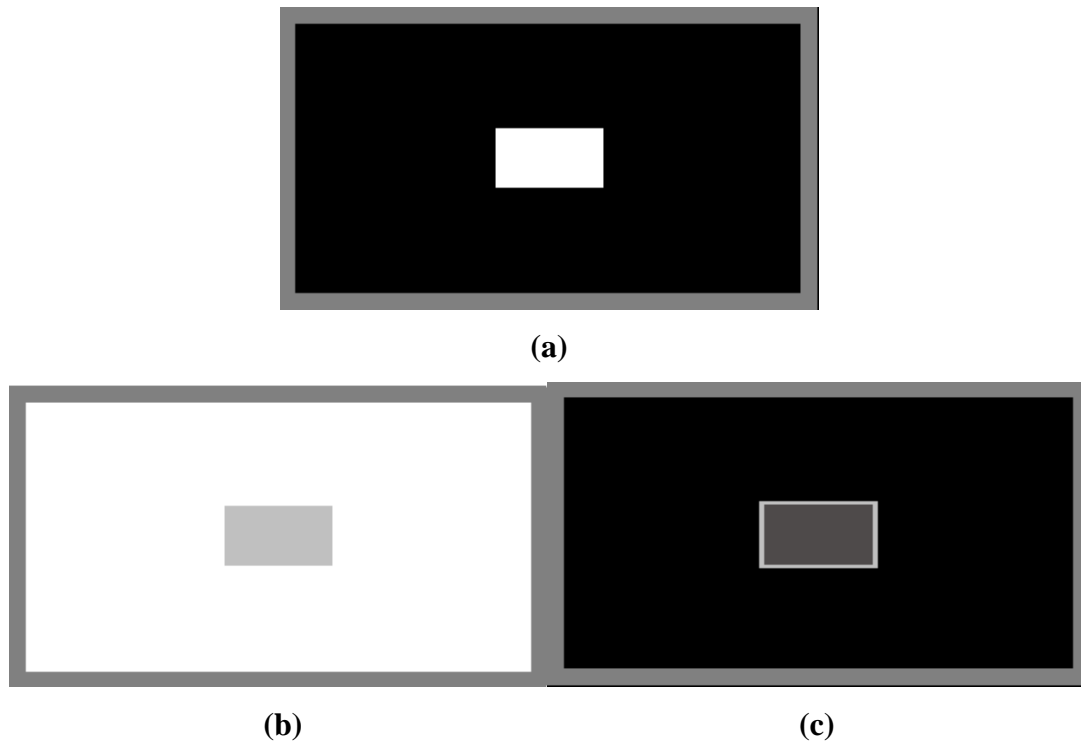


Fig. 5.12 (a) Photo diagram of the applied pattern (b) Photo diagram of the White Image sticking Phenomenon (c) Photo diagram of the Dark Image sticking Phenomenon

Tab. 5.2 Experiment panel setup

	Total Pressure	Xe partial pressure
1	475torr	6%
2	550torr	6%
3	475torr	9%
4	550torr	9%

5.3.2 Results and Discussion

In order to confirm the stability of the luminance and color performance in AC-PDP, the luminance variation of the conventional 46-inch panel was investigated. A full white 255 gray level image driving was applied on the panel after the power turns on. As one can see in Fig. 5.13, the luminance decay as a function of time and tend to remain stable 70 minutes later. It is believed that this phenomenon is related with the influence of temperature[4,6]. As the temperature of the phosphor arises, the emission efficiency from phosphor goes down. This phenomenon is so called temperature quenching effect of the phosphor. The higher surface temperature of the phosphor results in the higher probability that luminance center will get through

non-luminescent process with its absorbing energy dissipated in the form of heat[13].

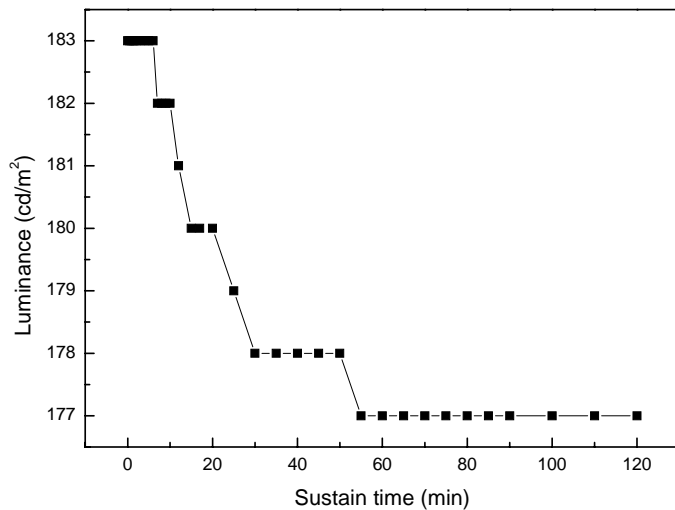


Fig. 5.13 Luminance degradation as a function of sustain time

Fig. 5.14 shows the luminance degradation as a function of time with different cells. Patterns with full red, green and blue color are applied on the panel after the power turns on. The luminance of each color also decays with time but remain stable after 70 min. It is noticed that the degree of luminance degradation is different with color, which is 4.7%, 4.8%, 4.4% for red, green and blue cells, respectively. The disparity among phosphors may result in color variation for AC-PDP. For this reason, the color temperature is recorded as a function of sustain time, as shown in Fig. 5.14d. It reveals that the color temperature also varies as a function of time. This phenomenon consists with the experimental results as Fig. 5.14a, 5.14b and 5.14c shown above. Since color performance corresponds to the properties of phosphors, it fits in with previous study that white image sticking phenomenon is to be caused by lower phosphor efficiency resulting from the higher temperature at phosphors[4].

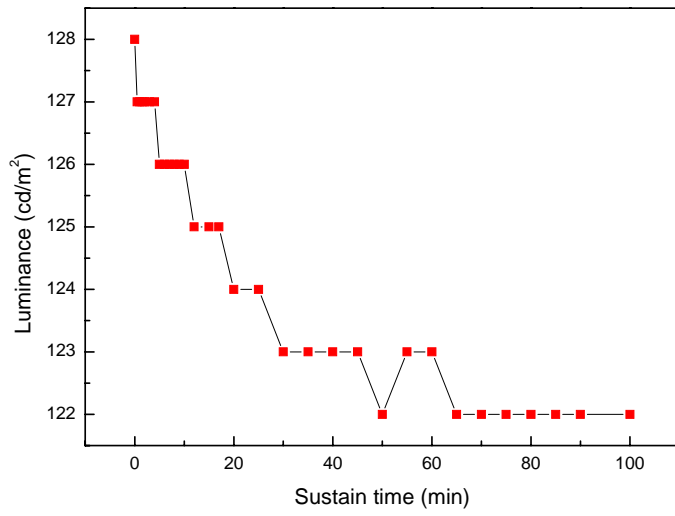


Fig. 5.14(a) Luminance degradation of the red cells as a function of sustain time

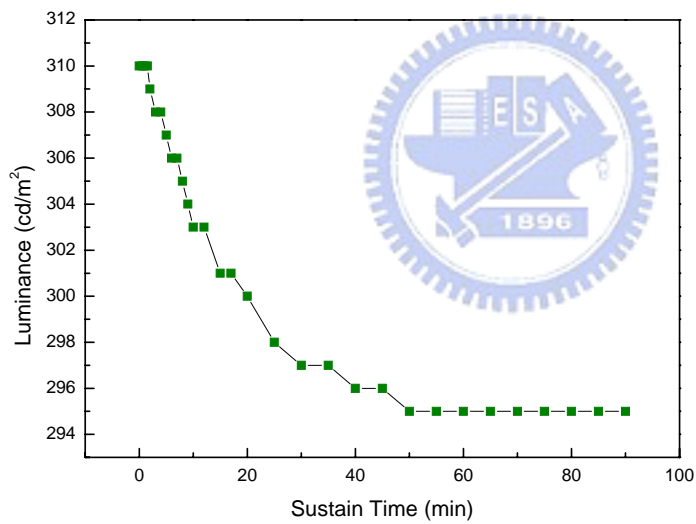


Fig. 5.14 (b) Luminance degradation of the green cells as a function of sustain time

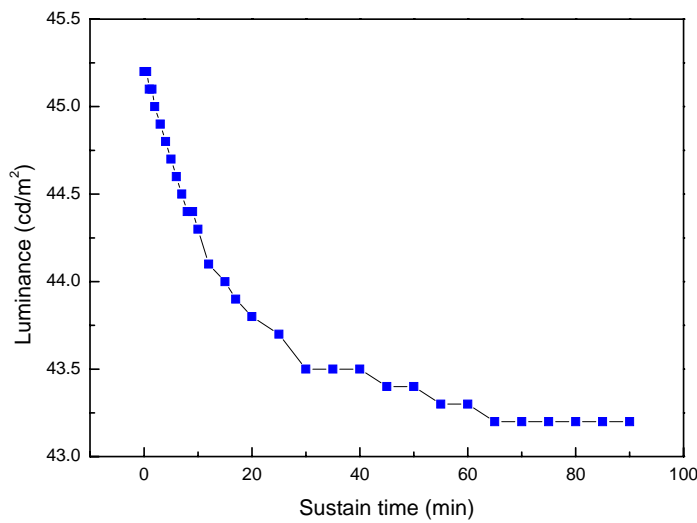


Fig. 5.14 (c) Luminance degradation of the blue cells as a function of sustain time

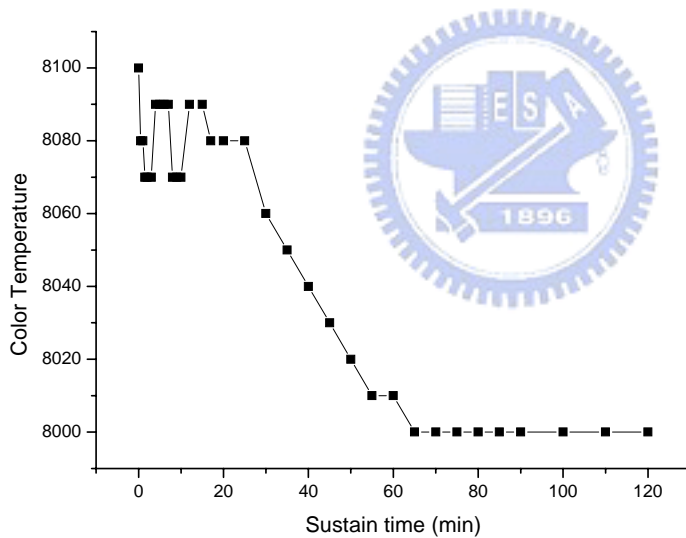


Fig. 5.14 (d) Color temperature variation as a function of full white display time

In order to investigate the degree of image sticking phenomenon, the recovery ability of the panels is needed to be introduced. Recovery ability is based on the time needed to recover from the image sticking condition to normal condition, which is, from the abnormal luminance or color performance to regular performance.

In this study, all data of recovery ability were measured after warming up the panels by full white displayed for 80 min to completely eliminate the effect of temperature

arising after power turns on, as previous section mentioned. Then a square-shaped white image was displayed for a period of time. After that, the pattern was changed to full area white displayed again to characterize the white image sticking phenomenon (WIS).

Fig. 5.15 shows the luminance of plasma display panel for different display times of square-shaped white image. The display pattern is the same as Fig. 5.12 (a) shows. The X axis in this figure means the display time of the pattern. After a period of display time, the display pattern changes to full white background and luminance degradation was measure at the position of square pattern, as Fig 5.12 (b) shows. The luminance at 0 time indicates the initial luminance of the panel. It reveals that the luminance difference increases on the increase of display time of square-shaped pattern. However it is relatively stable when the display time extends more than 10 minutes. The result indicates that temporal white image sticking phenomenon tend to saturate after 10 minutes successive static image displayed. It may caused by static surface temperature of phosphorous layer after long time display of the pattern area. Even though temporal white image sticking doesn't get worse after more than 10 minutes display, much longer pattern sustain time may cause permanent damage to the MgO films and phosphorous layer due to the strong iterant sustain pulse. It causes severer degradation for the pattern area and makes us hard to identify the recovery ability of the temporal image sticking phenomenon.

The recovery ability of the panels with different gas concentration and total pressure is shown in Fig. 5.16. In this case, the white pattern was displayed for 30 sec, 1 min, 2 min, 5 min and 10 min in the center of the panels. After that, the pattern was changed to full white background again to characterize the white image sticking phenomenon (WIS). The luminance variation of the image sticking cells in the square pattern area was recorded as a function of time. In the center of the panel, the luminance at 80 minutes warming up is considered as the standard value to compare with the values of the image sticking cells after square pattern displayed. An area near but outside the square pattern was selected to be the reference point also. However, the luminance of the area outside the image sticking area almost didn't change during the experiment. Each case was repeated multiple times to eliminate the experimental errors.

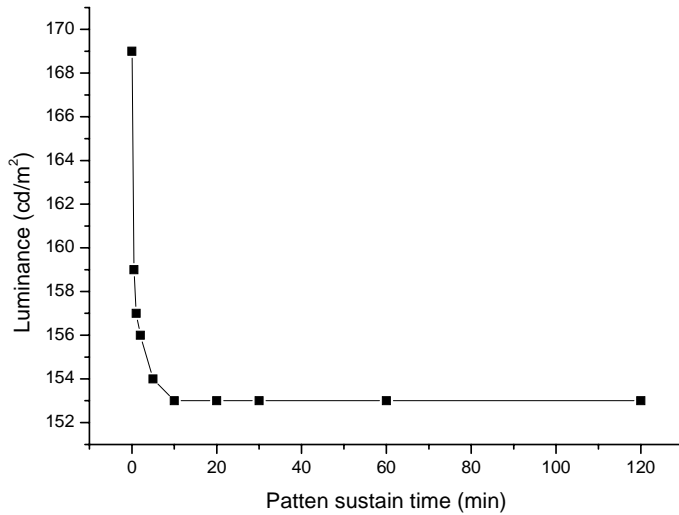


Fig. 5.15 Luminance degradation of the PDP after different pattern sustain time

As shown in Fig. 5.16, it proves that the PDP module with the conventional parameters (6% Xe gas ratio, 475 torr total inert gas pressure) exhibits superior recovery ability compared with the panels which include higher total pressure (No.2, 6% Xe gas ratio, 550 torr total pressure) or higher Xe partial pressure (No.3, 9% Xe gas ratio, 475 torr total pressure). For all cases in Fig. 5.16, the panel with conventional parameter (6% Xe, 475 torr total inert gas pressure) has less luminance difference than the other panels right after the pattern time, and recover to normal luminance in 2 to 5 min (slightly shorter than the others). For cases of 2min and 5min recovery time, the panel No.2 with 6% Xe gas concentration and 550 torr total gas pressure has higher luminance difference and longer recovery time than the panel No.3 with 9% Xe gas concentration and 475 torr total gas pressure. For case of 30 sec and 1min, the No.2 panel only has the longer recovery time than that of the No.3 panel. Furthermore, in all of cases the panel No.4 with higher Xe partial pressure (9%) and higher total pressure (6%) has the worst recovery ability, including the initial higher luminance difference and longer recovery time. Therefore, the higher Xe gas concentration and higher total gas pressure result in higher degree of white image sticking phenomenon. Furthermore, the influence of 550 torr is larger than that of 9% Xe partial pressure. Compared with the advantages of higher luminance and luminous efficiency at higher Xe partial pressure and total pressure, it revealed worse white image sticking characteristic, slightly.

It is not the result what we expected. The possible reason is discussed here. The high Xe partial pressure and high total gas pressure result in higher Xe excitation energy and higher electron heating efficiency, which make stronger VUV (Vacuum Ultra Violet) generation. Strong VUV achieves high luminance and high luminous efficiency of PDP. However, strong VUV also leads to high cell temperature. For conventional ac-PDP, the phosphor absorbs VUV and converted the energy into visible light emission. The main peak of VUV absorbed by phosphor is at 147 nm, 150 nm and 173 nm while the visible light is about 400 nm ~ 700 nm according to the colors emitted by phosphors. Therefore, the phosphor conversion efficiency is about 25% due to the wavelength difference of the VUV and visible light. The 75% energy is dissipated in the phosphorous layer as heat and results in cell temperature increase. Due to the temperature quenching effect of the phosphor, the phosphor efficiency decreases with the increased temperature. The temperature difference between the image sticking cell and non image sticking cell produces luminance difference between them. Therefore white image sticking occurs. That is why high Xe partial pressure and high total gas pressure make high luminance and high luminous efficiency but cause worse image sticking characteristic.

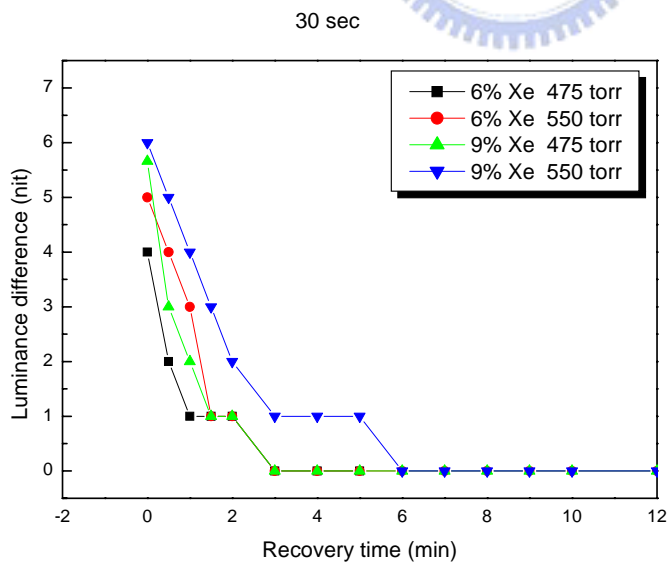


Fig. 5.16 (a) Recovery ability of the panels with 30 sec pattern sustain time

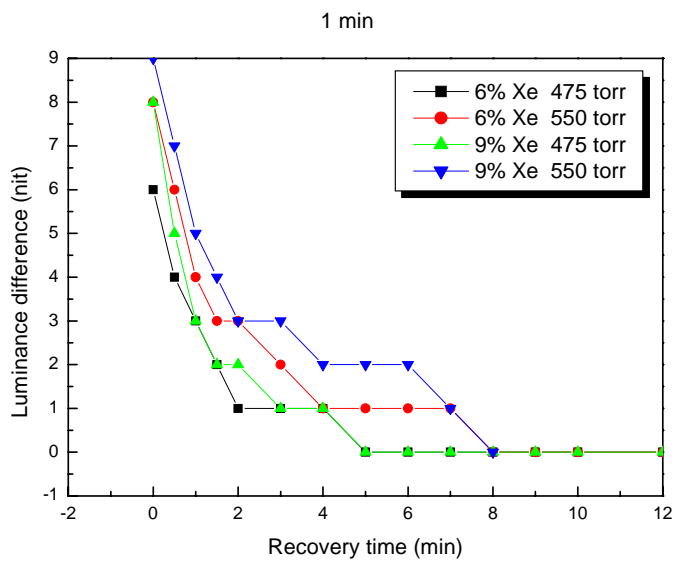


Fig. 5.16 (b) Recovery ability of the panels with 1 min pattern sustain time

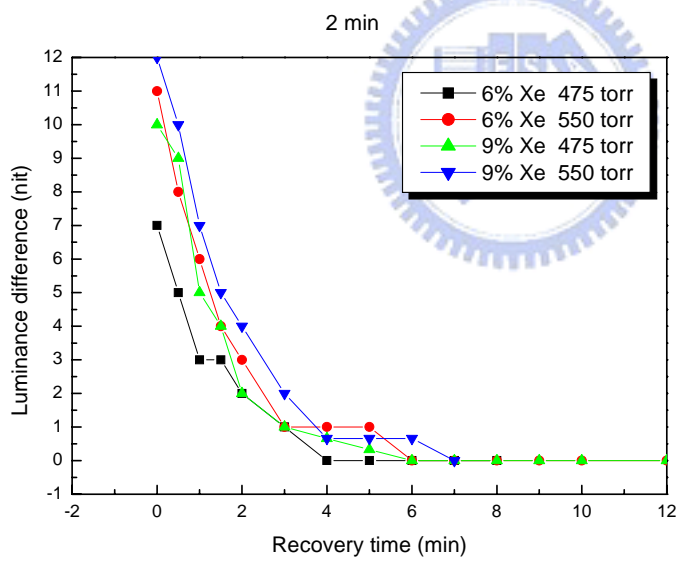


Fig. 5.16 (c) Recovery ability of the panels with 2 min pattern sustain time

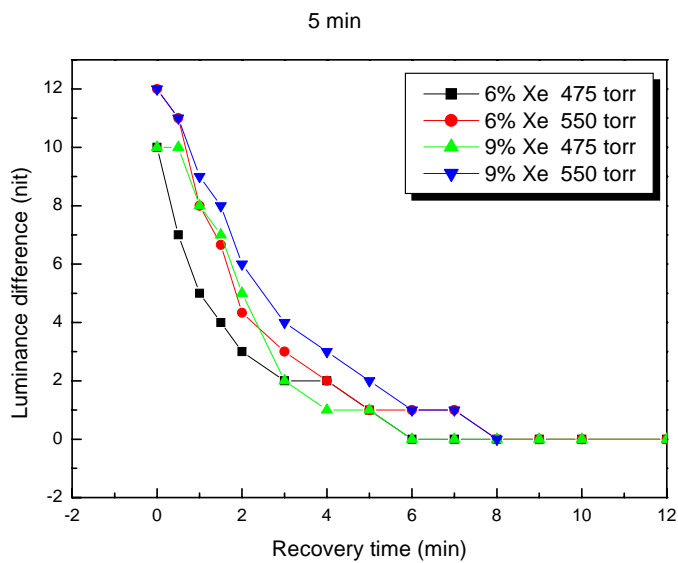


Fig. 5.16 (d) Recovery ability of the panels with 5 min pattern sustain time

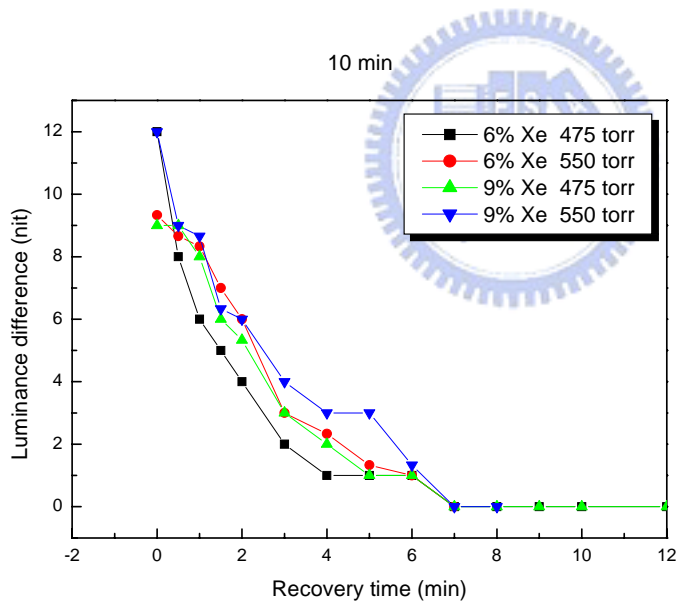


Fig. 5.16 (e) Recovery ability of the panels with 10 min pattern sustain time

5.3.3 Summary

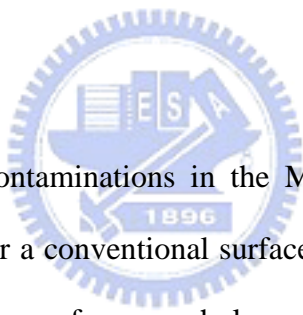
In this work, an image sticking observation of 46 inch WVGA AC-PDP was performed. The luminance degradation related to white image sticking phenomenon was investigated. The white image sticking phenomenon become more serious as a

function of Xe concentration (6%, 9%), and total pressure(475 torr, 550 torr). The effect of high total pressure (550 torr) is slightly more critical than that of high Xe partial pressure (9%).



Chapter 6 Conclusion

In this study, the degradation of MgO thin films and image sticking phenomenon were investigated. For the first part, several lifetime tests were proposed for MgO thin films in an ac-PDP. After long time operation, the driving margin area of the panel decreased. This is due to the degradation of MgO thin film by the ion bombardment in plasma. From the result, we found the panels with red phosphor have an obvious degradation. However, the Panels with green and blue phosphor only varied slightly. The driving margin is directly related to properties of MgO thin films. Therefore, we demonstrated that the degraded margin area is caused by contaminations in the MgO thin films by red phosphor.



In order to find out the contaminations in the MgO thin films, an accelerated lifetime test was performed for a conventional surface discharge type AC-PDP and a vertical discharge type one. The surface morphology and contaminations in the MgO thin films were investigated. By means of XPS, we confirmed that the element Yttrium, which is one of the main elements in the red phosphor, is contaminated in the MgO thin films of the vertical discharge type panel. This result consists with the result mentioned in previous section. We believe that the degradation of the MgO thin films in AC-PDP was partially caused by contaminations from phosphor. Even though the surface discharge type has stronger erosion on the MgO thin film because of long time discharge (16000 hr), there is no contaminations from the phosphor. It is difficult to detect the tiny amounts of the impurity and another method needs to be tried. The change of discharge characteristic in the MgO thin films can be an important property which needs to be studied.

In the second part, an image sticking observation of 46 inch WVGA AC-PDP was performed. The luminance degradation related to white image sticking phenomenon was investigated. The white image sticking phenomenon become more serious as a function of Xe concentration (6%, 9%), and total pressure(475 torr, 550 torr). The result may be due to the temperature difference between the image sticking cell and no image sticking cell caused by the strong VUV. For future work, it is essential to investigate the influence of higher temperature caused by inert gas setup with different driving voltage.



Reference

- [1] L. F. Weber, "The Promise of Plasma Displays for HDTV", SID '00 Digest, pp.402-409, 2000.
- [2] Ho-Jun Lee, Dong-Hyun Kim, Young-Rak Kim, Myoung-Soo Hahm, Don-Kyu Lee, Joon-Young Choi and Chung-Hoo Park, :“Analysis of Temporal Image Sticking in ac-PDP and the Methods to Reduce It”. SID2004, pp. 214.
- [3] Hirohito Kuriyama *et al.*, “High-Performance 55-inch Diagonal WXGA PDP with Extended ALIS Technology” SID 04 DIGEST, 2004
- [4] Heung-Sik Tae, Jin-Won Han, Sang-Hun Jang, Byeong-No Kim, Bhum Jae Shin, Byung-Gwon Cho, and Sung-Il Chien, :“Experimental Observation of Image Sticking Phenomenon in AC Plasma Display Panel”. IEEE TRANSACTIONS ON PLASMA SCIENCE, VOL. 32, NO. 6, DECEMBER 2004, pp. 2189.
- [5] Ho-Jun Lee, Dong-Hyun Kim, Young-Rak Kim, Myoung-Soo Hahm, Don-Kyu Lee, Joon-Young Choi and Chung-Hoo Park, :“Analysis of Temporal Image Sticking in ac-PDP and the Methods to Reduce It”. SID2004, pp. 214.
- [6] Jin-Won Han, Heung-Sik Tae, and Sung-Il Chien, :“Experimental Study on Temperature-dependent Characteristics of Temporal Dark Boundary Image Sticking in 42 in. AC-PDP”. SID2005, pp. 1036.
- [7] C.Koshio, H. Taniguchi, K. Amemiya, N. Saegusa, T. Komaki, Y. Sato, :“New High Luminance 50-inch AC PDPs with an improved Panel Structure using "T"-shaped Electrodes and "Waffle"-structure Ribs”. IDW'01, pp. 781
- [8] Seungho Choi, Soo-ghee Oh, Soonil Lee, Thin Solid Films 384(2001)115~119
- [9] Seungho Choi, Gilyong Shin, Hyunsuk Byun, Soo-Ghee Oh, Soonil Lee
Surface and Coatings Technology 169 –170 (2003) 557–561
- [10] J. E. Lim, W. B. Park, H. S. Jeong, K. B. Jung, W. Joen, H. J. Lee and E. H. Choi, IDW'04, pp. 1027.
- [11] Chung-Hoo, Park, Joon-Young Choi, Min-Suk Choi, Young-Kee Kim, Ho-Jun Lee, Surface & Coatings Technology 197 (2005) pp. 223– 228.
- [12] B. W. Jeoung, G. Y. Hong, B. S. Jeon and J. S. Yoo, IDW'02 (2002), pp. 809.
- [13] Shigeo Shionoya, William M. Yen, "Phosphor handbook", CRC Press LLC, New York, USA(1998)

- [14] Heung-Sik Tae, Sang-Hun Jang, Jin-Won Han, Byung-Gwon Cho, Byung-No Kim, and Sung-II Chien, :“Experimental Observation on Image Sticking of 42-inch PDP-TV”. SID2003, pp. 788.
- [15] G. Oversluizen, M. Klein, S. de Zwart, S. van Heusden, and T. Dekker, “Improvement of the discharge efficiency in plasma displays”. JOURNAL OF APPLIED PHYSICS VOLUME 91, NUMBER 4, 2002, pp2403.
- [16] M. F. Gillies and G. Oversluizen, “Influence of the noble gas mixture composition on the performance of a plasma display panel”. JOURNAL OF APPLIED PHYSICS VOLUME 91, NUMBER 10 15 MAY 2002, pp 6315.
- [17] Thibault Bignon, Pierre Boher, Véronique Gibour and Thierry Leroux, “Image Sticking Cartography on PDP TV: A New Quantitative Measurement”. SID2005, pp. 598.
- [18] Jin-Won Han, Byung-Gwon Cho, Heung-Sik Tae, and Sung-II Chien, :“Design of Facing Reset Discharge Waveform for Reducing Dark Image Sticking in AC-PDP”. SID2004, pp. 532.
- [19] T. Onimaru, S. Fukuta, T. Misawa, K. Sakita, K. Betsui, SID2004, pp. 1241.
- [20] R. Kim, Y. Kim, J. W. Park, Thin Solid Films 376 (2000), pp. 183–187.
- [21] S. O. Kim, Journal of Vacuum Science and Technology B, Volume 21, Number 1, pp. 233–236.
- [22] Shuxiu Zhang and Heiju Uchiike, IDW '02, pp. 689.
- [23] T. Onimaru, S. Fukuta, T. Misawa, K. Sakita, K. Betsui, IDW '02, pp. 693
- [24] H.K. Hwang, C.H. Jeong , Y.J. Lee , Y.W. Ko , G.Y. Yeom, ”Effect of plasma cleanings on the characteristics of MgO layer for plasma display panel”. Surface and Coatings Technology 177 –178 (2004) 705–710
- [25] Shinji Tadaki, Kazunori Inoue, Shinya Fukuta, Manabu Ishimoto, and Keiichi Betsui, “Analysis of Deterioration of $\text{BaMgAl}_{10}\text{O}_{17}:\text{Eu}^{2+}$ Phosphor for Plasma Display Panels”. SID2001, pp. 418
- [26] Tae Wan Choi, Jin Young Kim, Seong Ho Kang, Jeong Jun Kim and Hyung Kyun Bae, ”Influence of MgO Protecting Layer on the Response Time in AC-PDP”. SID 2000, pp. 748